Photo irradiation experiments and its effects on lifetime and degradation of blue PolyLEDs

Colditz, H.J.O.

Award date:
2005

Photo irradiation experiments and its effects on lifetime and degradation of blue PolyLEDs

H.J.O. Colditz

The research was done at
Philips Research Laboratories
Eindhoven, The Netherlands

in order to achieve the degree of
Master of Science
at the
Eindhoven University of Technology.

The graduation project was supervised by
Dr. R. Kurt, Philips Research
(Group Large Area Devices & Instrumentation)
and
Dr. ir. M. Kemerink, Eindhoven University of Technology
(Molecular Materials and Nanosystems, faculty of Applied Physics)

Preface

All the experimental work done and the experiences gathered working ten months at the group Large Area Devices & Instrumentation part of the sector Materials & Process Technology at Philips Research Laboratories are part of my graduation project at the department of applied physics at the Eindhoven University of Technology.

Unfortunately, but also understandable, this report shows only part of the research performed. It focuses on the major results that contribute to the primary research objective. Due to the limited time of my stay and other practical circumstances not every interesting detail could be further investigated or reported. But then, that was not the aim of this report. Nevertheless, if any questions about this report arise, I would be happy to try to answer them or to provide additional information if possible.

Abstract

PolyLED displays suffer from a loss in luminance efficiency during normal operation, resulting in limited device lifetimes. This is especially the case for the blue light emitting polymer (LEP). So far it was considered that the electrical an optical degradation mechanisms are identical. Therefore irradiation experiments could provide insight in the degradation process. Many experiments were performed involving several light sources within the visible spectrum to study systematically parameters like the photon energy and the duration and intensity of irradiation. Depending on the wavelength of the irradiated photons two different effects were observed: one caused by photons with energies within the absorption band of the LEP and surprisingly also one caused by photons with energies below the absorption band of the LEP. Degradation effects for low energy photons are induced by the presence of the cathode, whereas high energy photons also interact with the bulk of the LEP. Furthermore, irradiation could unexpectedly be used in a way to slightly improve device lifetimes. From the findings it can be concluded that the mechanisms behind photo-degradation are not identical to the mechanisms behind electrical degradation.

Contents

1. Introduction

In this chapter the motivation and background behind the research presented in this report is set out. It starts off with a brief overview of the current status in the field of polymer Light Emitting Diodes (PolyLEDs) and some of the current issues related to the field of physics. Finally, the aim of this research project is explained.

1.1. Brief historical overview

The first reports concerning electroluminescence of an organic semiconductor go back to the mid 1960s [1]. Luminescence was observed on organic crystals when applying a few hundreds volts [2]. In the 1990's large academic and industrial interest was established when the electroluminescence from a thin polymer film (at about 10 Volt) was reported by Richard Friend and co-workers because of the possible applications in display technology [3]. Since then a lot of research has been directed towards the development of new efficient polymeric emitters. A whole range of polymeric LEDs, emitting over the whole visible wavelength region from red to blue, has been reported. Furthermore, the PolyLED performance was greatly improved, by the introduction of additional charge-transport layers.

Interest is still being stimulated by the technology's intrinsic advantages such as processing ease, low cost and the design flexibility of the technology affords (including the possibility of producing, e.g. flexible displays). Alongside these advantages is the fact that the technology is capable of combining the functions of light-emitting diode and photo diode in a single device, allowing the integration of multiple functions in a display, e.g. touch screen and display, comprising just one active layer. A PolyLED display has several strong features, e.g. high contrast, isotropic emission leading to viewing angles approaching 180 degrees and high brightness. The PolyLED technology is very energy efficient and lends itself to the creation of ultra-thin lighting displays that will operate at lower voltages. This makes the PolyLED suitable to become the new generation of high-quality displays.

1.2. Current issues

Nowadays, the first commercial applications of monochrome polymer LEDs are a fact, and research focuses on the development of full-colour polymer displays. However, the fabrication, processing and efficiency optimisation of three different polymers for the three basic colours (RGB) is rather difficult. To circumvent these problems a substantial research effort is put into the incorporation of dye molecules in one basic polymer layer and to improve lifetime and efficiency for each separate dye molecule. But, despite the rapid progress in the field of polymeric light-emitters, no full colour displays based on polymer LEDs are commercially available yet. The long-term device stability and device efficiencies of polymer LEDs are increasing, but improvements are still desired, especially for polymers emitting in the blue wavelength region. The main challenge for commercialization of polymer based LEDs in the field of displays is the operational lifetime of the device. Currently lifetime values for blue polymer LEDs lie in the range of about 100 to 1000 hours, whereas the benchmark for consumer displays, for example, is in the range of 10.000 to 100.000 hours.

Various industrial and academic groups around the world are performing research on the cause of performance loss over time of full colour displays. Most of the work is naturally focussed on blue polymer LEDs. The change of performance is referred to as degradation. Understanding the

processes behind degradation is seen as an essential step in order to slow it down or even annihilate these unwanted effects.

As a result, research at Philips has also focussed on the study of degradation phenomena of blue polymers. Part of Philips' research is to study the processes that cause these devices to degrade and, when understood, to practically solve the underlying problems technologically.

1.3. Aim of research

As mentioned, a thorough understanding of the complex physics behind a properly working PolyLED is strongly required. Several aspects of the PolyLED in the field of physics have already been put in theoretical modelling. Degradation is not fully understood yet. One aspect is the interaction of light with a PolyLED, another is the electrical degradation, which will not be focussed on in this study. Degradation is suggested to be partially caused by photons generated by the device itself or by interactions of the photons with excited states or charge carriers in an operating device. This part of the degradation process is often referred to as photo-degradation. The aim of this research is to provide input from an experimental point of view to the understanding of photo-degradation and to modelling of a PolyLED, specifically at room temperature conditions. In doing so, characterization of the effects of light on device performance is needed and a major part of the study reported here is focussed on this. Off course any direct contribution to improving the lifetime of a PolyLED is a welcomed extra from the applicational point of view.

2. Theoretical background

This chapter will give a short overview of polymer Light Emitting Diodes (PolyLEDs) with regard to the research performed for this report. Conjugated polymers will be introduced, followed by the operating mechanism and built-up of a PolyLED and finally some ideas about the parameter space of photo-degradation this study deals about.

2.1. Conjugated polymers

Electroluminescence from conjugated polymers was already reported in 1990 [3], using poly(*p*-phenylene vinylene), PPV, as the single semiconductor layer between metallic electrodes.

In conventional polymers every carbon atom in the backbone is single-bonded (σ-bond) to four atoms in the sp^3 hybridized configuration. The difference with a conjugated polymer is that three of the four electrons in the outer shell of carbon occupy sp^2 hybridized states, creating the σ-bonds that form the strong structural backbone of the polymer. The remaining free electron occupies a p_z orbital. The equivalent p_z orbitals from neighbouring carbon atoms overlap and form the so-called π-bond. Therefore conjugated polymers are represented by a framework of alternating single and double carbon–carbon bonds. In reality, the electrons that constitute the π-bonds are delocalized over the entire molecule [4]. This is known as electron delocalization. Although this process costs lattice energy, because the double bonds are shorter than the single bonds, the gain in electronic energy, due to an opening of an energy gap of about 1.5 to 3.5 eV between filled bonding states (the Highest Occupied Molecular Orbital (HOMO) states or valence band) and the empty anti-bonding states (the Lowest Unoccupied Molecular Orbital (LUMO) states or conduction band) is larger [5]. This energy gap makes the polymer a semi-conducting material.

2.2. Operating principle of a PolyLED

PolyLED displays form one application area of conjugated polymers. A polymer-based LED consists of a single layer of a fluorescent polymer sandwiched between two electrodes, one of which is transparent. In general, the conjugated polymer must perform three functions: hole transport, electron transport and light emission. A schematic energy-level diagram for a PolyLED device under forward bias is shown in figure 1.

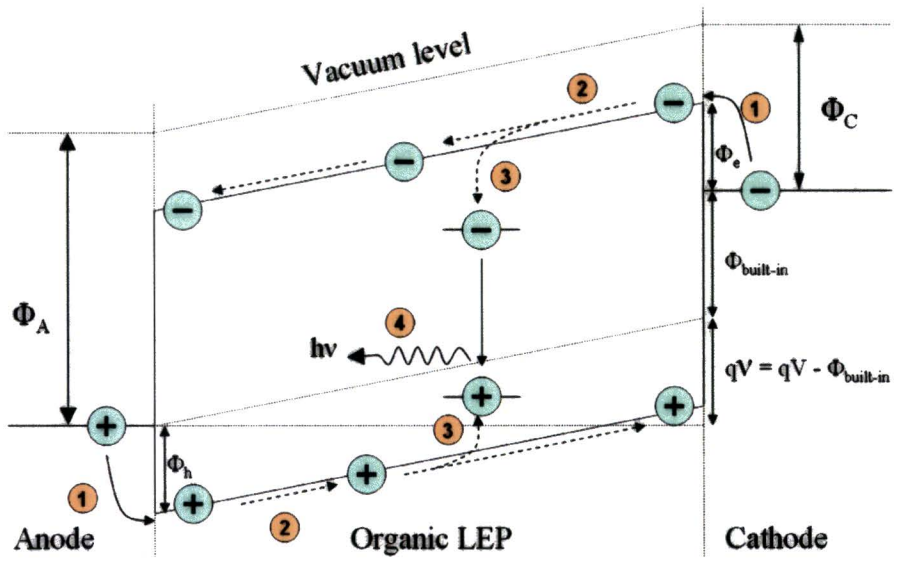

Figure 1: Schematic energy level diagram for a PolyLED. In numbers the basic steps for electroluminescence are indicated: (1) charge carrier injection, (2) charge carrier transport, (3) exciton formation, (4) radiative exciton decay. Φ_A: anode work function, Φ_C: cathode work function, Φ_h: hole injection barrier, Φ_e: electron injection barrier, $\Phi_{built-in}$: built-in potential, q: elementary charge, V: applied voltage, $\mathcal{V}$: effective voltage across the organic layer. Picture based on original from [6].

By applying a voltage between the anode and cathode, i.e. the two electrodes of the PolyLED, electrons (-) and holes (+) are injected from cathode and anode respectively as illustrated in figure 1 and figure 2. The injected charges migrate through the organic semiconducting layer, mainly by hopping from polymer chain to polymer chain but also along the chain and under the influence of the applied electric field they obtain a drift velocity. When charges of opposite sign meet each other in the vicinity of a single conjugated segment, they can combine and they will form neutral bound excited states (referred to as excitons). There are two types, singlet and triplet excitons, with an occurrence ratio of 1:3 due to spin statistics. In the light emitting material used in this work only the singlet state decays under the emission of a photon.

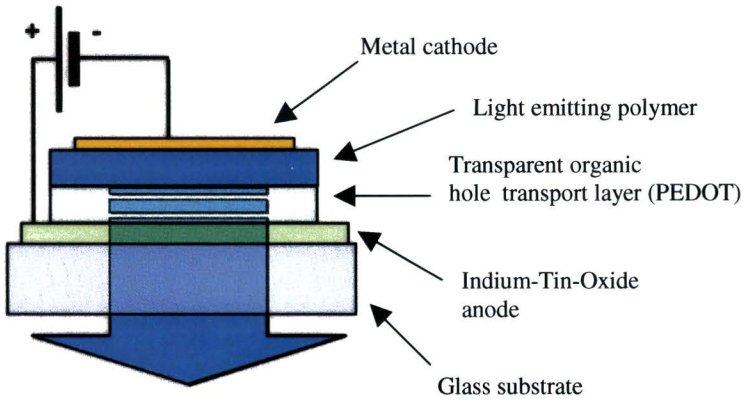

Figure 2: Schematic cross section of a PolyLED pixel. Electrons that recombine with holes within the polymer contribute to light emission.

Under open-circuit potential conditions (OCP), i.e. no applied voltage (V=0 in figure 1), holes are collected at the high work function anode (Indium-Tin-Oxide, ITO), and electrons are collected

at the low work function cathode. This is due to the work function difference $\Phi_{built\text{-}in}$ between the two electrodes, which gives rise to an internal electrical field.

A combined experimental–theoretical approach to the study of polymer surfaces and interfaces has been applied to a wide variety of conjugated polymers and model molecules, as well as to the early stages of metal-on-polymer (and model molecule) interface formation [7], [8]. They showed that the nature of interfaces, between the active light-emitting polymer medium and the metal electrode, or between the polymer and the ITO layer, are of importance in determining device performance, apart from the properties of the layers itself.

2.3. PolyLED display built-up

The PolyLED devices studied were fabricated in the Philips Research pre-pilot line at the High Tech Campus Eindhoven. In this study standard devices (as schematically depicted in figure 3) were made on glass substrates covered with a structured ITO anode layer. On top two layers were spin coated: a hole conduction polymer layer (PEDOT:PSS=poly(ethylene-dioxythiophene):poly(styrenesulfonate), about 100 nm) and a light emitting polymer (LEP, about 80 nm). In this work exclusively samples comprising the standard blue light-emitting polymer* used by Philips were studied. On top of the spin coated layers first Barium (5 nm) and then Aluminium (100 nm) were evaporated. This Ba-Al layer acts as the cathode. The ITO and PEDOT are used as an anode. In figure 3 the cathode can be electrically connected on the right side of the drawing, whereas the anode can be connected on the left side.

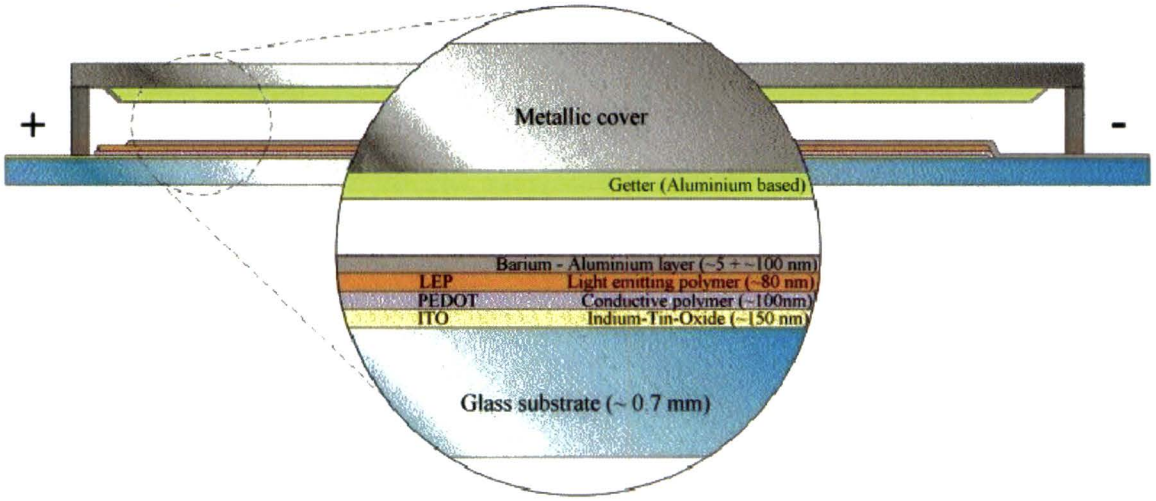

Figure 3: Schematic view of the cross section of a PolyLED sample showing the layered structure (not on scale)

Spin coating of the PEDOT and LEP layer was done in a clean environment under normal atmospheric conditions. Evaporation was done in a vacuum chamber to prevent oxidation of the reactive cathode material. All devices were packaged under protected nitrogen atmosphere using a glued metal cover and a getter was placed inside the obtained cavity. The getter ensured that oxygen and water degassing from one of the components or due to leakage did not play a role in the degradation processes studied in this work. The cavity itself contains dry nitrogen (N_2).

* Because of reasons of confidentiality the name or chemical structure cannot be presented here.

The experiments were performed exclusively using the so called multipixel design nr.PL0072C. That means each sample has multiple light-emitting areas, called pixels. All pixels have the same structure of layers as mentioned above, but some differ in size. A top view of a device is shown in figure 4 and the light emitting areas are numbered and shown in blue.

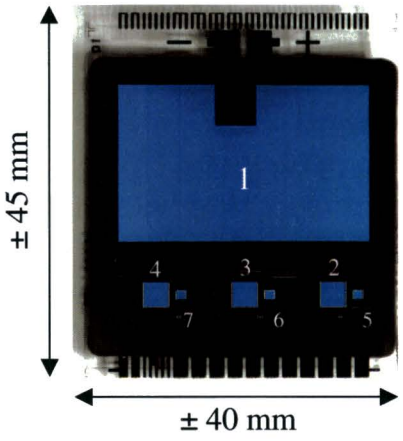

Figure 4: Top view of PolyLED sample, showing in blue several areas called pixels. In white numbers the pixel referring convention is specified.

The size of the pixels 2, 3 and 4 (as defined in figure 4) is 3 mm by 3 mm, i.e. 0.09 cm^2. Pixels 5, 6 and 7 have a surface area of 1 mm^2 and pixel 1 has a surface area of 5.25 cm^2. The sample shown in figure 4 is cut out of a 6 inch by 6 inch production plate with nine samples. One production batch consists of three of such plates, resulting in 27 samples per batch.

2.4. Parameter space of photo-degradation

There is evidence that electrical stress causes much slower degradation in single charge carrier devices (electron only and hole only) compared to double carrier devices like the studied PolyLED [9]. So, degradation also occurs in devices that show no light emission at all. In double carrier devices charge carriers, several excited states and photons are all simultaneously present in the light emitting polymer (LEP) under normal operating conditions.

The focus in this study lies on effects on lifetime due to photons interacting with the device and their contribution to the degradation process. Especially photons with energies and a spectral distribution like the photons emitted by the device itself are of interest. Since the LEP emits photons with energies within its own absorption band, additional excited states are being generated possibly contributing to degradation of the device. To study interactions of photons, three different external light sources with different techniques and analysing methods were used to irradiate PolyLED devices. They will be explained in the following chapters.

As the PolyLED degradation is generally linked to the driving conditions of a PolyLED during operation the parameters involved in operating a device might be of interest for this study. In figure 5 the parameters selected to be of importance for this work are illustrated and they will be explained next.

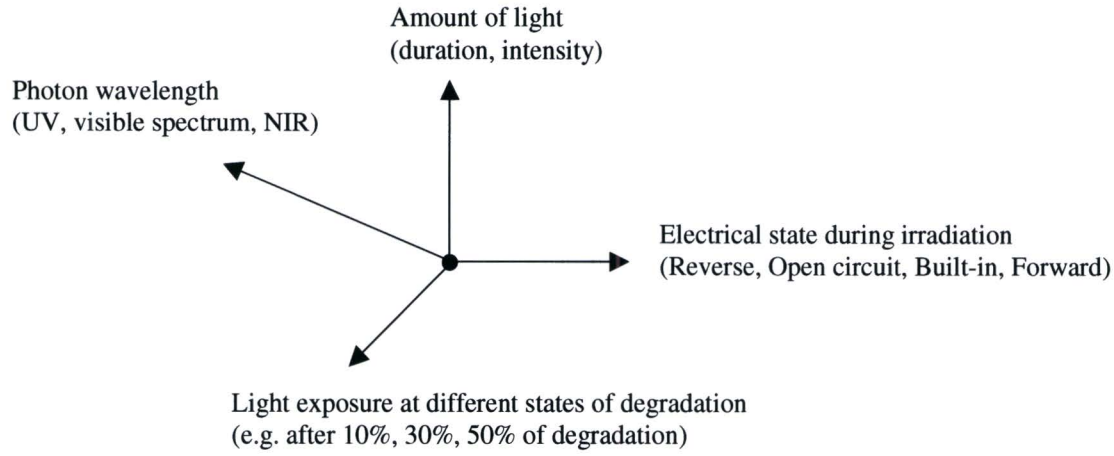

Figure 5: Schematic illustration of the parameter space selected to be of importance for study in this work.

As a working hypothesis, it was suggested that excited states are potentially interacting with photons and contributing to the degradation process [10]. So, the electrical state of the device with regard to photo-degradation is an interesting parameter to study.

Secondly, the degradation due to electrical stress may be directly linked to the process of photo-degradation. So the mechanisms of photo-degradation might be different for different stages during the lifetime of a display.

Furthermore, the amount of light involved with photo-degradation is of interest. Both the duration and intensity of illumination, or the combination of both, i.e. the dose, could be of importance. One could for instance expect threshold or saturation phenomena.

Next, the wavelength of the photons involved with photo-degradation is of interest. Photons with higher energies are expected to contribute more to degradation. However, photons with specific wavelengths or energies may be favourable for some degradation processes. Certainly, since the energy of blue photons (up to 3eV) is in the range of the binding energy of the chemical C-C-single-bond, i.e. about 3.6eV.

Finally, there may be other parameters of importance, e.g. boundary conditions due to the design of the display and the materials used.

Moreover all the parameters mentioned could all influence each other and many complicated degradation processes are thinkable. However these four listed parameters were studied in detail and only the conclusive and major results are presented.

3. Instrumentation and experimental setup

3.1. Standard lifetime setup

For the characterisation of luminance and voltage, samples were measured in a standard lifetime set-up at the Reliability Centre. The samples were placed in standard holders and kept at room temperature in a temperature-controlled environment. The samples were electrically connected to a computer to control and monitor voltage, current and luminance over a long period of time. The luminance was measured by a pre-calibrated photodiode, which is an integral part of the sample-holder. Samples were operated in constant-current mode. Typically one computer could control up to 48 samples simultaneously, using Labview software.

3.2. IVL-characteristics

For the electrical characterisation before and/or after lifetime or irradiation experiments current, voltage and luminance (IVL) characteristics were measured in a set-up which is also part of the Reliability Centre. A Keithley 2400 source meter is used to apply a voltage over the PolyLED sample and to measure the corresponding current. Simultaneously a Keithley 617 programmable electrometer is used to record the electroluminescence (EL) by a Si photodiode. Each apparatus is connected to a computer and controlled by a Labview software package in order to measure a sample automatically and reproducibly.

3.3. Irradiation - Suntester equipment

At the Reliability Centre new equipment was prepared for illumination experiments. The apparatus used was an Atlas Suntest XLS/XLS+ with a UV-special glass filter (illustrated in figure 6).

Figure 6: Photographic image of the Atlas Suntest XLS/XLS+ showing the reflective radiation chamber.

The new equipment was used to build an experimental set-up like the available standard lifetime set-up. The same calibration methods and software packages were used.

The radiation chamber of the suntester was slightly adapted for our purpose and new dedicated sample holders were made so samples could still be connected to standard controlling and monitoring computers of the Reliability Centre, i.e. experiments with simultaneously illuminating and electrically driving the samples became possible. In order to get more cooling power a Sun-Cool air-cooling unit was also attached to the suntester. This made it for the first time possible to get room-temperature-like conditions in the radiation chamber for experiments. Previous experiments [10] at similar suntest machines were done at about 50°C or even higher temperatures which caused numerous problems. Normally the suntester was operated at maximum power (765W/m² irradiance across the horizontal test plate on which the samples were laid) and maximum cooling (15°C air temperature). The spectral power distribution of the lamp in the range of 280nm-3000nm (as depicted in figure 7) is a good approximation of sunlight at sea level and satisfies the requirement of CIE (Pub. No. 85, Table 4).

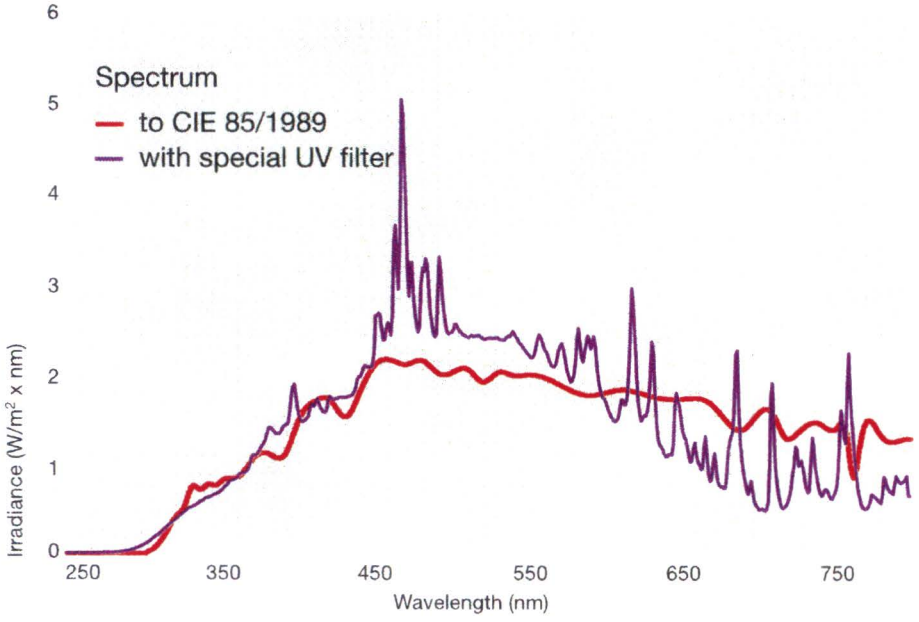

Figure 7: Spectral distribution Suntest XLS/XLS+ plotted against wavelength (data taken from [11]). The purple line is the irradiance incident on a sample. The red line is the empirical irradiance for sunlight at sea level.

Several glass filters were available to select an interesting wavelength regime for our investigations. They matched the dimensions of the samples and could simply be placed on top of them. It turned out that light bypassing the filters and coupling in sideways through the glass substrate influenced the experiments, so in order to protect samples from this, special metallic reflective covers were made with a small opening to let light irradiated the designated area (illustrated in figure 8).

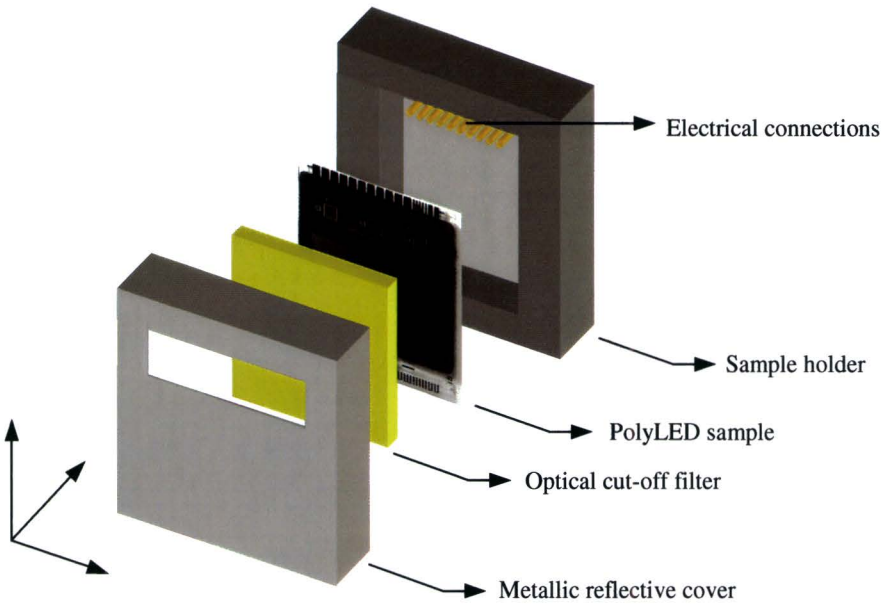

Figure 8: Exploded view of the positioning of a sample in relation to its holder, cover and filter, as used in the suntest set-up.

The sample temperature was monitored automatically by the suntester and represented by the so called Black Standard Temperature (BST). However, our samples were no black bodies and therefore temperatures could be different. In addition always one thermocouple was placed between the cover and one of the samples. From both temperature measurements it can be concluded that the sample temperature was between 18°C and 25°C.

3.4. Irradiation - Optical rainbow set-up

As an alternative way to study the effects of wavelength dependence the so called "rainbow set-up" was built as part of my work. Basically the light of a white light source was diffracted by a grating into a complete continuous spectrum (illustrated in figure 9). In appendix B an introduction to the theoretical background about blazed diffraction gratings is given. The optical system of the rainbow set-up also comprised a collimator and a lens in such a way that the entire visible spectrum was focused to cover the total width of the large pixel 1 of a standard multipixel device.

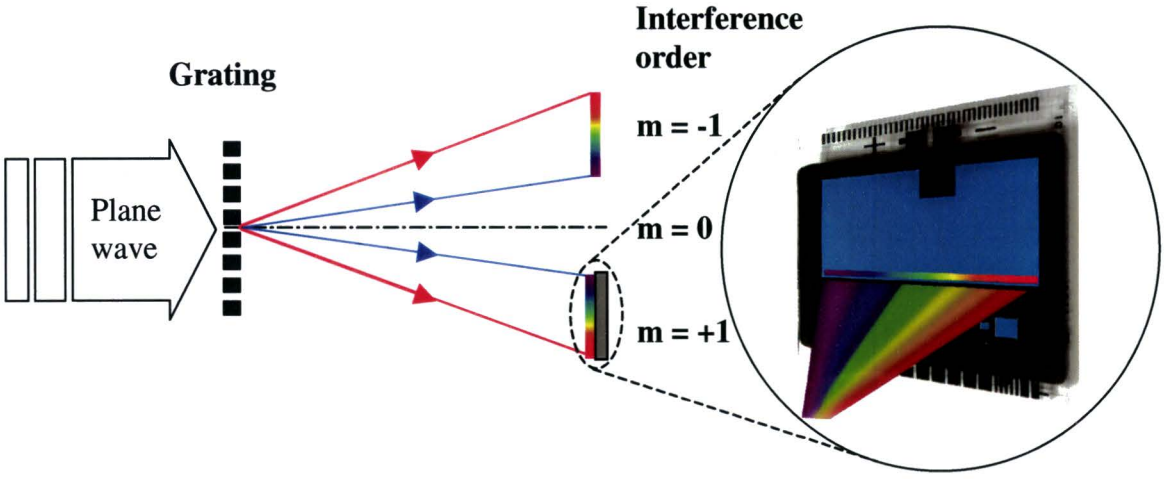

Figure 9: Schematic overview Rainbow set-up. The inlet shows in perspective how the beam is projected onto the largest display pixel of the sample. In the actual experiments a reflective grating (explained in appendix A) was used, but not shown here for reasons of clarity.

For the white light source a Schott KL1500 150 Watt halogen cold light source was used. The spectral power distribution of the lamp is shown in figure 10.

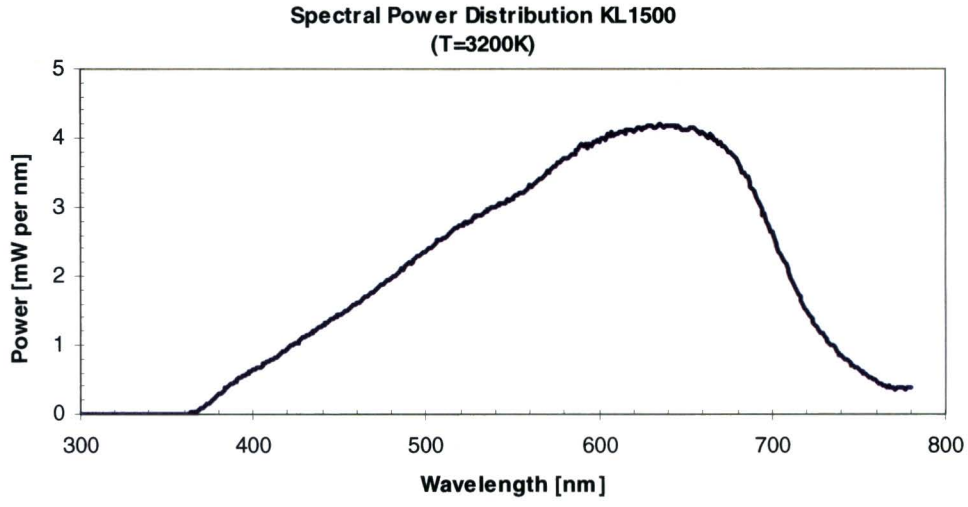

Figure 10: Spectral power distribution of the Schott KL 1500 as function of wavelength.

In the actual experiments a set-up like the so called Littrow mount [12], [13] was used. This involved a reflective plane diffraction grating with 1200 grooves/mm and a blaze angle of 4°. The grating had an optimal efficiency at λ_B=500nm for first order (m=1).

Filters were placed in the path of the light in order to select different regions of interest from the full visible spectrum. In all the experiments a 400nm cut-off filter from Schott (GG400) was used and from appendix B we can calculate that in this case this leads to a free spectral range F of 400nm. So, the whole visible spectrum (400nm-800nm) in principle could be used for our experiments. The total area covered by the rainbow was about 1.7mm by 30mm and the irradiation power incident on the sample in first order (m=1) was about 1mW (400nm-800nm).

3.4.1. 8-bit CCD-camera

Any inhomogeneity in a pixel makes the interpretation of a standard IVL-characteristic very difficult. As it turns out, partial irradiation of a large pixel of the PolyLED causes localized inhomogeneities. Measuring the overall current density, as is done in all the previous standard characterisation methods, is not very useful because it could vary significantly as function of position.

However, taking a high resolution image of a whole pixel emitting light at a specified current showed, at least qualitatively, the effect of localized irradiation over a large wavelength range. A set-up was made with an 8-bit CCD-camera connected to a computer and controlled by the software package Image-Pro Plus. Normally pictures were taken when the sample was driven by a current density of 1.74 mA/cm^2 (or actually, simply 10mA for pixel 1). In addition a UV-lamp was installed so photoluminescence (PL) pictures could be taken as well.

4. Analyzing methods

One of the main focuses in studying the effects of photo-degradation was to compare samples before and after illumination experiments and also to compare them to so called reference samples. These reference samples had a similar history in electrical stress, but were kept in dark, so no effects of external light sources were present.

4.1. Batch variation

A big challenge lies in dealing with the variation of properties and performances of samples from within one batch. Hereby is meant that samples that were made in the same production process still had different electrical and optical characteristics. This is largely caused by inhomogeneities and variation of thickness of one or more of the layers of the PolyLED. Additionally the properties of the devices are known to be very sensitive to tiny production process parameter changes.

4.1.1. Normalization

For studying the optical characteristics typically luminance efficiency curves were plotted. The luminance efficiency is calculated from the measured luminance [cd/m²]. Dividing the luminance by the applied current [A] and then multiplying by the surface area [m²] of the studied pixel leads to luminance efficiency. In order to annihilate some of the effects of batch variation a normalization procedure in the standard lifetime set-up was performed for each sample. In figure 11 the absolute and normalized luminance efficiency of three similar samples are shown. In the left figure the spread of signals makes it difficult to compare the mutual differences in behaviour over time. After normalisation (right figure) identical behaviour can be easily recognised because the data points of different samples fall substantially on top of each other.

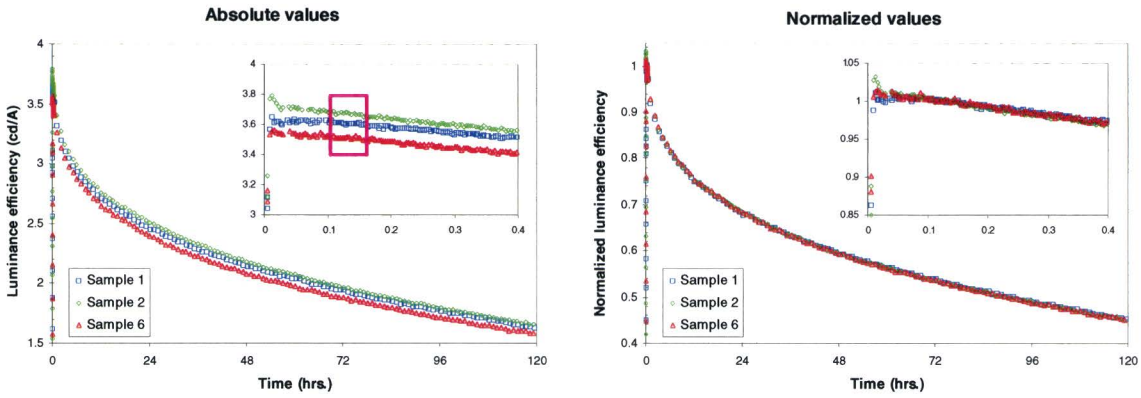

(a) *(b)*

Figure 11: Typical lifetime curves (lifetime curves are explained in 4.3) for absolute (a) and normalized (b) luminance efficiency vs. time. The inlets show the first 0.4 hours of the measurement. In (a) a spread of signals from similar samples (represented by red, green and blue data points) within one batch is observed. In (b) each signal was normalized to the average value within the purple box shown in (a); after normalization the three efficiency curves fall substantially on top of each other and are considered to behave identical.

The normalization procedure consisted simply in applying the typical current for that particular experiment for 10 minutes, after which the actual experiment was done. From these data the average value of the observed parameter (e.g. efficiency, voltage) between 5 and 10 minutes was taken to be the normalization value 1. The period from 5 until 10 minutes is rather arbitrarily chosen. It should be a few minutes after start-up, due to start-up effects, but not much longer due to early stage degradation effects. The 10 minutes mark is also used for the standard characterisation procedure used by the Reliability Centre.

4.1.2. Statistical averaging

Normalized data from lifetime experiments sometimes varied significantly. These variations occurred from batch to batch, from sample to sample and even from pixel to pixel. There may be several reasons for the occurrence of these abnormalities, e.g. shortcuts, inhomogeneities or bad electrical contacts. Normally irregularities in the luminance efficiency characteristics corresponded to those in the voltage characteristics (in 4.3 the efficiency and voltage characteristics are explained). However in some cases, only irregularities in one plot of the lifetime curves were observed. In either case the data was not reproducible and therefore not further analysed. In order to get enough reliable data for interpretation and also for reasons of reproducibility, most of the experiments were done with three or four similar samples simultaneously, preferably from within one batch. Sometimes several samples within one experiment showed abnormalities, in which case the experiment was redone with a new set of experimental samples and reference samples.

In the Rainbow set-up however, it simply was not possible to measure multiple samples simultaneously. Therefore, sample numbers #2, #4, #6, #8 from one batch-plate were preferred. Normally samples corresponding to these locations on a batch-plate turned out to have the best homogeneous layers after spin coating. Even from this selection only the best samples with good enough homogeneous EL over a large area were used for experiments. Without this selection procedure noise signals, inhomogeneities, dark spots, light spots, minor spin-coating defects, etc. would make interpretation of the line scan method (4.4.1) very difficult.

4.2. Reference samples

Reference samples were used to rule out shelf and hold effects in general. They were always taken from the same production batch as the samples on which the light-exposure experiments were performed. Reference samples were kept under dark conditions but were subjected to the same electrical stress as the samples used in experiments with external light sources (e.g. suntest). And again, for reasons of statistics and reproducibility, always three or four reference samples were used simultaneously.

When comparing the properties of the samples, this procedure ensured that the effects caused by irradiation with light could be well separated from other possible effects and therefore reliably studied.

4.3. Analyzing typical lifetime curves

By lifetime curves generally the relationship between luminance efficiency [cd/A] and time at constant electrical stress is meant, but sometimes it is also referred to voltage versus time curves

at constant electrical stress. These lifetime curves are recorded in the standard lifetime set-up or suntester set-up as previously described. In chapter 5 several of these curves will be presented and discussed. In order to get acquainted with the typical characteristics and terminology used, the important aspects for understanding will be discussed in the following paragraphs.

4.3.1. Experimental procedure

The typical experimental procedure for the lifetime set-up or suntest set-up is schematically illustrated in figure 12.

Figure 12: Schematic overview of the different phases a sample goes through in a typical experiment using the suntest set-up or lifetime set-up. Time is on the horizontal axis, the widths off the phase-blocks are not drawn proportionally scaled to each other.

A sample goes through four phases:

1. Preparation, cleaning and calibration of the luminance of the sample at the desired current density used in phase 4. The samples are electrically stressed for calibration for about 3 seconds.

2. Characterization of the luminance efficiency and voltage properties at the desired current density that will be used later in phase 4. The data is used for normalisation (duration of electrical stress at characterisation = 10-12 minutes).

3. Experimentation phase. During this phase the actual experiments took place. All samples were placed in the irradiation chamber of the suntest set-up in special holders with optical cut-off filters. References samples were kept under dark conditions by covering them with a highly reflective mirror instead of the filter. Many experiments were done at so called open circuit potential (OCP), i.e. the sample is electrically disconnected, but also experiments with simultaneous irradiation and electrical stress were performed (duration of this phase depended on the experiment and could be less than one hour or up to a hundred hours).

4. Lifetime characterisation phase. Now that the history of reference samples and samples used for irradiation experiments is different, the electrical and optical properties are characterised in a standard lifetime experiment. These characterisations are normalised to the data from phase 2 (the duration of this phase takes at least as long as it takes to reach the 40% luminance efficiency value of the normalisation data from phase 2, normally more than hundred hours).

At the end of phase 4 samples are simply stored under dark conditions at room temperature. The time between phases was kept as short a possible. However, several experiments involved up to 27 samples, so time between phases 2 and 3 or 3 and 4 could take up to several tens of minutes, due to e.g. handling, electrically connecting and starting the samples.

4.3.2. Normalized luminance efficiency lifetime curve

One of the main important degradation observables is the behaviour of the luminance efficiency over time. The luminance efficiency [cd/A] is obtained by dividing the measured luminance [cd/m²] from the photodiode by the applied current [A] and then multiplied by the surface area [m²] of the studied pixel. The calculated values are normalized to the characterization data from phase 2 and are shown in figure 13. There are two important areas used for studying the characterization data.

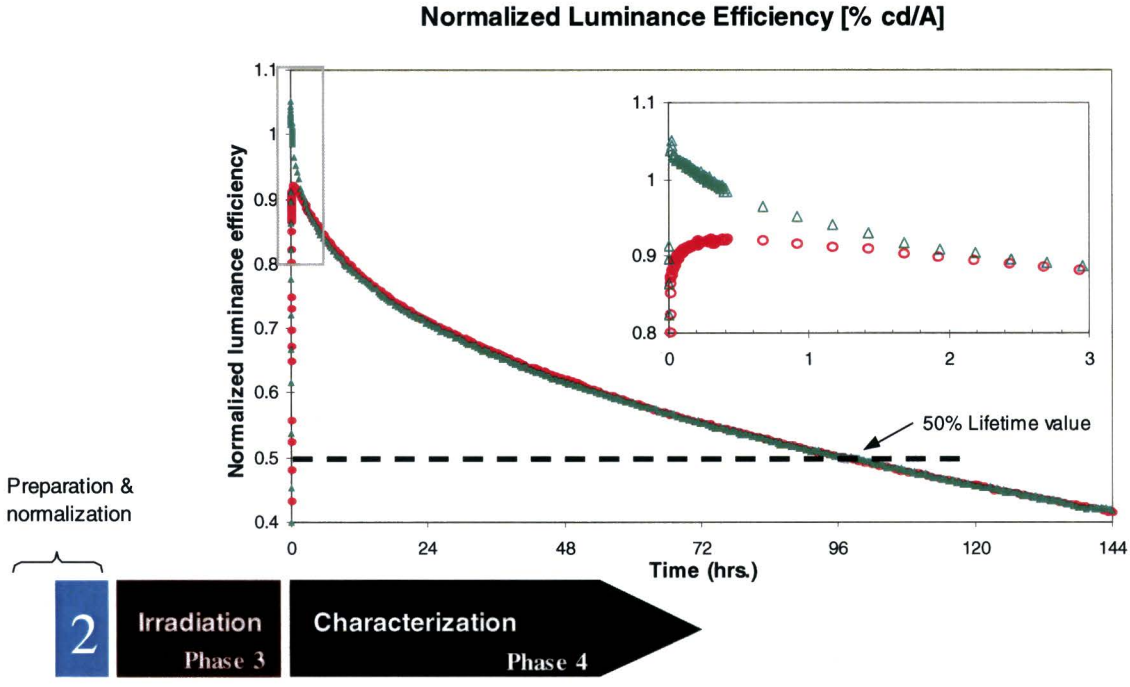

Figure 13: Normalized luminance efficiency versus time at constant electrical stress after 24 hours of irradiation at OCP. In red typical experimental data after irradiation is shown, the green data belongs to a corresponding non-irradiated reference sample. The inlet shows the first three hours (indicated with the small grey box) where an initial offset is observed. The time at which the efficiency curve reaches the value 0.5 marks the 50% lifetime value. In this case the lifetime is about 99 hours. For practical reasons the origin of the time axis is shifted to the start of phase 4, as indicated with the arrow at the left bottom.

The first region of interest is the initial behaviour of the luminance efficiency in phase 4 compared to a non-irradiated reference sample, shown as an inlet in figure 13. The second region of interest is the behaviour at 50% of its original value as measured in the normalization phase 2. The details of the characteristics shown in figure 13 will be discussed later in chapter 5. Although generally the history of a sample is of importance for interpreting the data, normally the data from phase 1-3 will not be plotted in this report and the origin of the time axis will be shifted to the start of phase 4. In principle the samples with red and green data points had a similar history regarding electrical stress during phase 1-3 and only effects due to irradiation in phase 3 should be the cause of differences in phase 4.

4.3.3. Voltage lifetime curve

The second important degradation observable is the behaviour of voltage over time, as shown in figure 14. The voltage is measured simultaneously with the luminance.

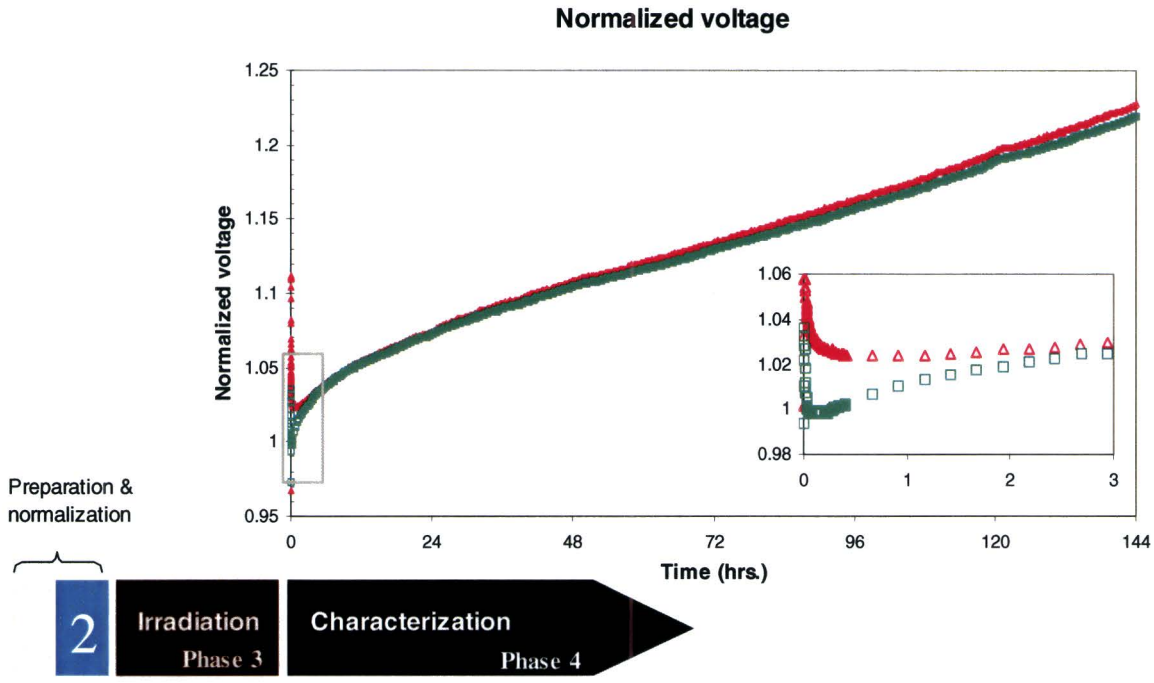

Figure 14: Normalized voltage versus time at constant electrical stress after 24 hours of irradiation at OCP. In red typical experimental data after irradiation is shown, the green data belongs to a corresponding reference sample. The inlet shows the first three hours (indicated with the small grey box) where an initial offset is observed. For practical reasons the origin of the time axis is shifted to the start of phase 4, as indicated with the arrow at the left bottom.

Here too, the same two areas are important for characterization: one on the short term, as shown in the inlet of figure 14, the other on the longer term, around the 50% lifetime value extracted from figure 13.

Care has to be taken when interpreting the initial off-set, which may, apart from irradiation effects, also be due to a bad electrical contact when reconnecting the sample in phase 4. Due to operating the samples in constant current mode there are no additional effects caused by such contact-resistances in the luminance efficiency curves.

4.4. Analyzing with the 8-bit CCD-camera

Samples from the rainbow set-up were photographed using an 8-bit CCD-camera and analysed with the Image-Pro Plus software package. The main characterisation method used was newly developed and is referred to as line scan profiling.

4.4.1. Line scan profiling

Images taken with the CCD-camera were digitalized into 256 grey values. These values correspond to the luminance of the photographed object. Comparing a previously irradiated area to a not irradiated area (as shown in figure 15) provided information about the effects of irradiation. The non-irradiated areas were normally also covered by black tape for additional shielding.

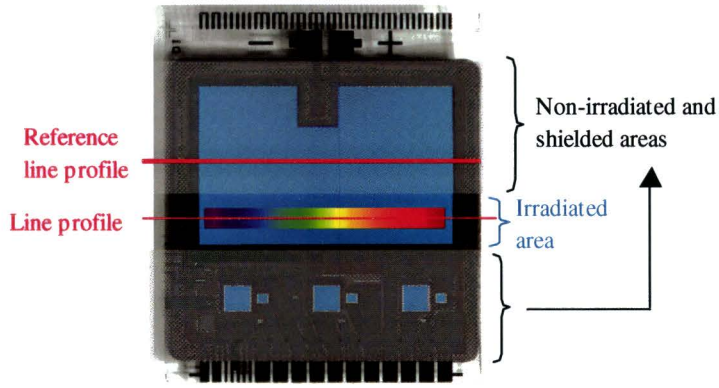

Figure 15: Schematic overview of line profiling. The digitalized luminance (or grey values) as function of position on the red line through the irradiated area is compared to the values of a line profile in the non-irradiated part of the pixel.

To minimize noise signals and the effects of local irregularities several line profiles next to each other were taken and averaged.

4.4.2. Calibration scale

The second step in analysing a sample that was irradiated by different wavelengths as function of position (as is done in the rainbow set-up) is to make a conversion from a particular position to the corresponding wavelength of the light that irradiated that position.

Due to the fact that each PolyLED sample had slightly different dimensions of the glass substrate after cutting free the nine samples from one production plate and different samples could not be placed at exactly the same spot, care had to be taken to be sure what wavelength irradiated what position of the sample. Therefore, always a second experimental procedure involving an interference filter (Schott BG35) was done on the same sample, slightly above or below (vertically shifted to) the previously irradiated area (illustrated in figure 16).

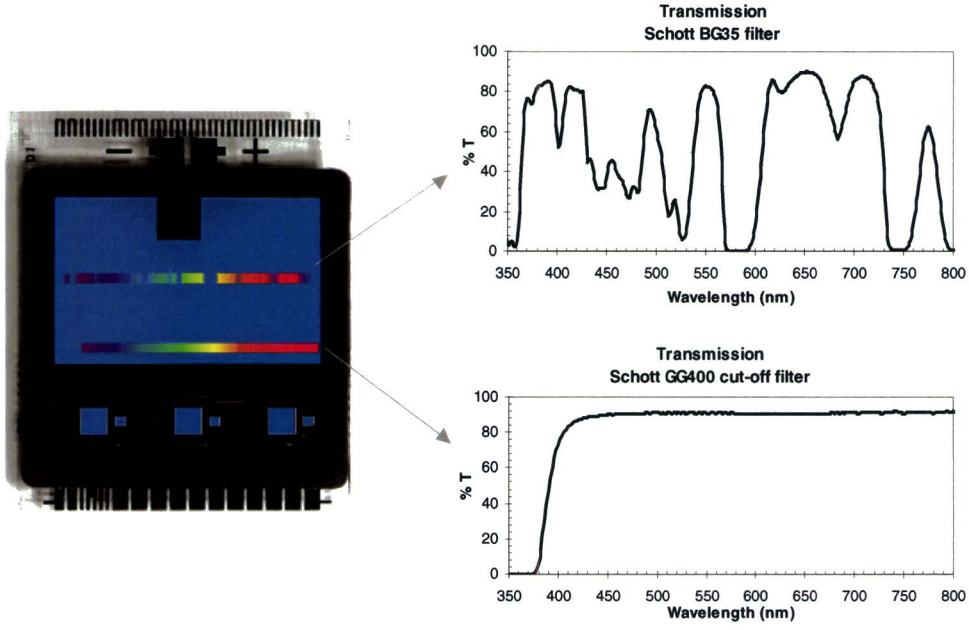

Figure 16: Schematic illustration of a PolyLED irradiated twice with a rainbow spectrum of visible light: upper strip irradiated with an interference filter (BG35) to calibrate the wavelength axis, lower strip with the full spectrum (>400nm) for the actual wavelength analysis. On the right the transmission vs. wavelength curves of the used filter for each strip are shown. As a consequence for the upper strip, certain areas will be less irradiated than others.

It turned out that the EL-spectrum of irradiated areas did not change, so no care was taken for the spectral sensitivity of the camera.

5. Experimental results

Only a selection of all the experiments performed are presented here. The selection was done by focusing on the major findings. These findings represent reproducible data.

5.1. Typical sample properties

Before studying and comparing effects of irradiation, first some basic measurement results of typical properties of the samples used are shown. The basic built-up of a PolyLED sample has already been described previously. The standard light emitting polymer* (LEP) used by Philips Research with a layer thickness of 80nm is used in all the experiments.

In figure 17 the measured spectral radiance (blue curve) and the absorption spectrum (grey curve) of a standard blue emitting PolyLED device are shown.

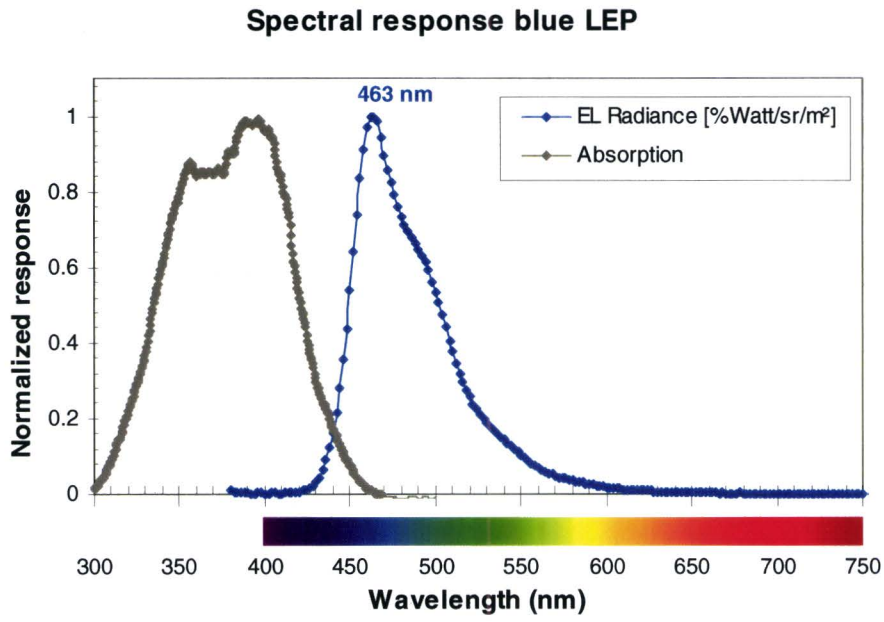

Figure 17: Normalized radiance (blue) and absorption (grey) vs. wavelength of a standard sample. The blue electroluminescence curve reaches it maximum at 463 nm. On the horizontal axis also the visible colour spectrum (from 400nm to 750nm) is shown for illustration.

From this measured absorption spectrum we see that apart from the desired blue light also other colours are emitted. Furthermore, the absorption band overlaps the electroluminescence (EL) band. So, a normally operated device will create excitons by photo-absorption of its own emitted light. Below 425nm less than 1% is emitted and above 460nm less than 1% is absorbed.

Apart from the optical properties, the electrical properties (as depicted in figure 18 and figure 19) are of major importance. The typical diode like characteristic can be clearly recognised. The luminance efficiency curve (blue data in figure 18) shows us that light is only produced at voltages larger than the built-in voltage created by the energy work functions of the (cathode and

* Because of reasons of confidentiality the name or chemical structure cannot be presented here.

anode) materials used in the PolyLED, in this case at 2.4V. The built-in voltage also marks a distinct point in the current-voltage (IV)-curve (red data in figure 18). The applied electrical field below the built-in potential, i.e. 2.4V, is too small to generate sufficient current in the LEP-layer and the data is regarded to be leakage current and its behaviour is considered ohmic. Above the built-in voltage the behaviour is no longer ohmic and also a small hysteresis effect is observed, although this is not clearly visible in the logarithmic plot.

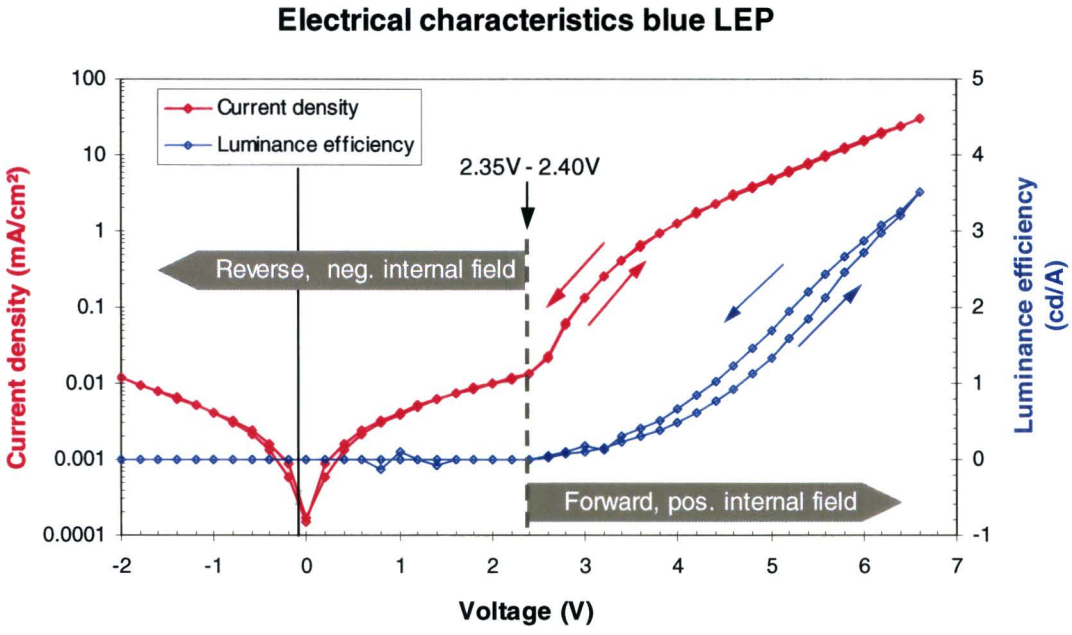

Figure 18: Current density (red, log scale, left axis) and luminance efficiency (blue, linear scale, right axis) versus voltage. Hysteresis is observed when voltage is increased and then decreased, arrows indicate the direction. For the negative current density values (at negative voltage) the absolute values are plotted, because of using a log scale. At voltages larger than about 2.4V (built-in potential) light is produced in the PolyLED and can be seen by the eye or recorded by a photodiode.

Figure 19 shows the relation between luminance and current density. The relationship is roughly linear at values larger than 100 cd/m², which simplifies the conversion between the two physical quantities.

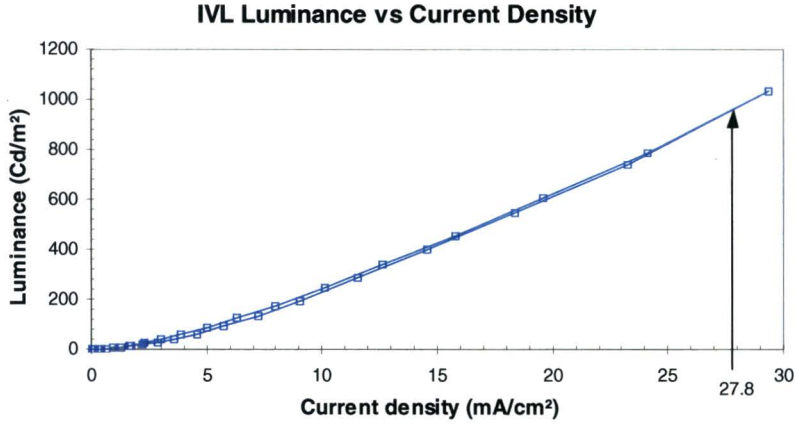

Figure 19: Luminance versus current density. The relation is almost linear above 100 cd/m². Typical values for display applications range between 100 cd/m² (CRT), 250 cd/m² (LCD) and up to 600 cd/m² for high end televisions. The arrow indicates the current density used in most experiments for operating the device.

Most of the experiments done in the standard lifetime set-up or suntest set-up were performed at a current density of 27.8 mA/cm² (≈1000 cd/m²). This resulted in an accelerated degradation process and was done for practical reasons.

In figure 20 typical luminance efficiency lifetime curves of new, untreated and non-irradiated samples, so called virgin samples, are shown. These measurements were always made to check whether a new production batch was representative compared to other batches. The experiments simply consisted of a calibration, i.e. phase 1 as explained in section 4.3.1, and a long characterisation, i.e. phase 2, with a constant current density of 27.8mA/cm².

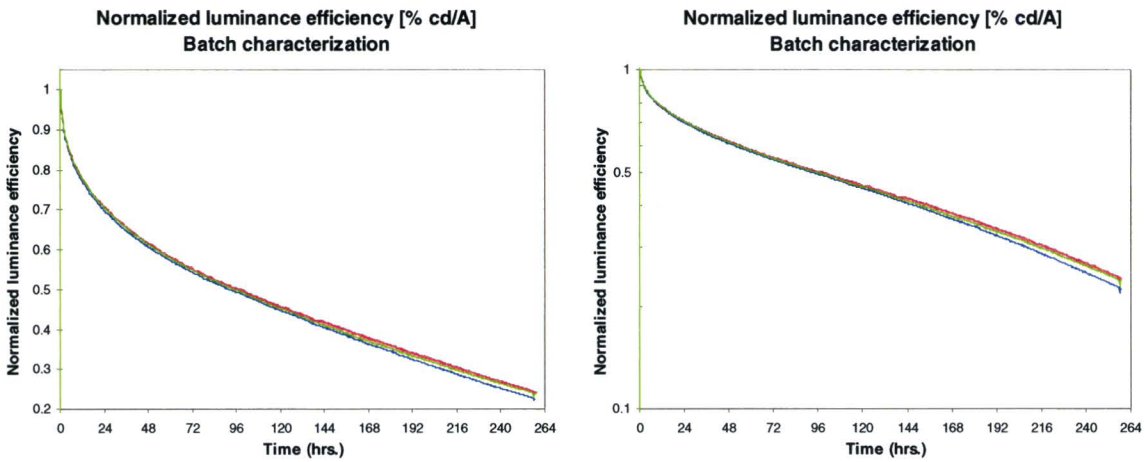

(a) *(b)*

Figure 20: Normalized luminance efficiency versus time operated at constant current of three similar virgin samples (red, green and blue) from one production batch plotted on linear scale (a) and logarithmic scale (b). The plotted loss of efficiency over time is referred to as degradation of the PolyLED. Initially a fast degradation is observed. The data points of the three samples virtually fall on top of each other down to 40% of its initial value. From that point on sample variation within one production batch, e.g. due to different layer thickness, non-uniformities, etc. becomes distinguishable.

First of all, figure 20 shows that efficiency reduces steadily over time. This reduction of efficiency at constant current results in a reduced brightness of the display and is referred to as degradation of the PolyLED display. Three different stages of degradation are shown in figure 20 and can be distinguished best in (b). First a phase of fast degradation in the first hours (roughly 24 hours in this case), then a phase of much slower degradation well beyond the 50% lifetime value and finally again a somewhat faster degradation after about 200 hours. This last phase, where also the efficiency of identical samples start to behave differently, is out of the scope of this study. The first degradation phase can be influenced by light, as will be shown in the following sections. This first fast degrading part resembles 'initial drop' behaviour as reported earlier [14]. The degradation due to light will be referred to as photo-degradation.

5.2. Suntest irradiation

Unless mentioned otherwise, studying irradiation effects in the Atlas Suntest XLS/XLS+ was always done on one of the 3 mm by 3 mm pixels (shown in figure 4, pixel 2, 3, 4) of a sample. The bias used for measuring an accelerated lifetime curve (phase 4) was 2.5mA, i.e. 27.8 mA/cm². The same current density was used in phase 1 and 2 for calibration and normalization. Irradiation always occurred at maximum power of the suntester, i.e. 765W/m² between 300-800nm.

First the results of a rather simple experiment with important results will be shown. This will answer one of the important questions, namely if light and in particular light irradiated by the display itself, does have an effect on the performance of a PolyLED and simultaneously it will familiarize us with the used terminology, boundary conditions and typical results.

In the following experiments samples were pre-characterized (phase 2), then irradiated with a broad wavelength range (solar spectrum) at high intensity (phase 3) and finally again characterized (phase 4). The different phases are illustrated in figure 21.

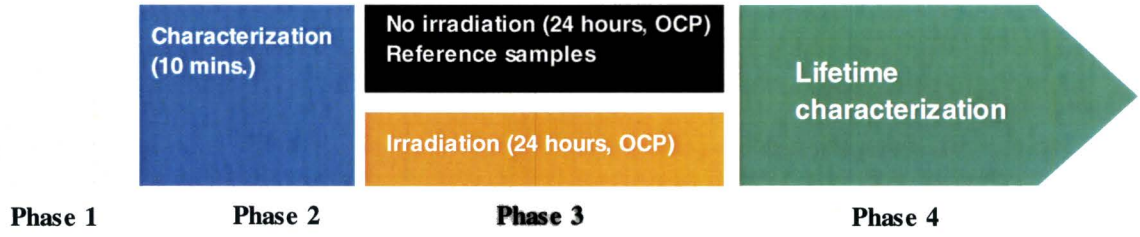

Figure 21: Schematic overview of the phases of electrical stress a sample goes through in a typical suntest irradiation experiment used for lifetime characterization after irradiation. Reference samples were not irradiated in phase 3 but were subjected to the same electrical stress as experimental samples.

It is well known that irradiation in the absorption band deteriorates performance and harms the efficiency of a PolyLED [10], but this is not part of this study so therefore cut-off filters (Schott GG435) were used to filter out wavelengths smaller than 435 nm. Samples in the suntester were not electrically connected (Open Circuit Potential mode = OCP). Irradiation lasted in this case for 24 hours (phase 3). Correcting for the use of the GG435 filter, this resulted in homogeneous irradiation of about 5 mW for the studied pixel, integrated over the suntest spectrum from 435nm to 800nm. After irradiation the lifetime curves were measured (phase 4). Figure 22 shows the typical change of behaviour in the lifetime curves compared to not irradiated reference samples.

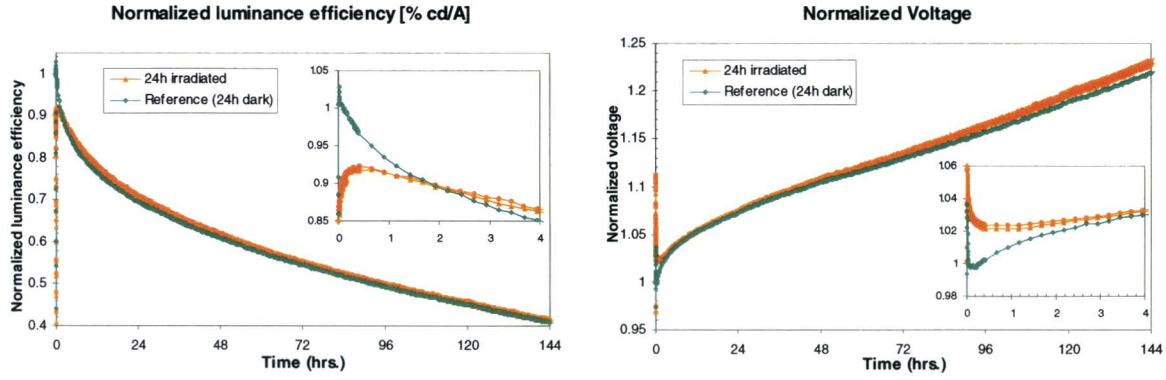

Figure 22: Normalized luminance efficiency (left) and normalized voltage (right) lifetime curves operated at constant current density (27.8 mA/cm²). The inlets show in more detail the first 4 hours of the response. The green data represents a reference sample without irradiation and the same electrical history as the orange data. The samples corresponding to the orange data were irradiated for 24 hours in OCP-mode, only two data lines are shown for clarity. The data from 3 reference samples virtually coincide, but only one green data line is plotted for clarity. The lines between points are intended to guide the eye along the data points.

One of the most obvious effects is the initial drop or offset in luminance efficiency and voltage when comparing the irradiated samples to reference samples. However, within a few hours the efficiency of the irradiated and non-irradiated samples approach each other after this initial drop phase. Important to note is that on the long term these two characteristics are almost identical, for instance the 50% lifetime value, i.e. about 93 hours, is virtually unchanged. Also the behaviour of

normalized voltage on this timescale has hardly changed. For reasons of clarity only one green and one orange curve is plotted, but the characteristics are reproducible although normally a spread in signals, due to sample to sample variations, does occur.

From these results it can be concluded that light outside the absorption band of the blue LEP does interact with the PolyLED devices. What follows in the next paragraphs is to take a closer look at the influences of different irradiation times, different electrical conditions of the samples and what part of the spectrum of light is causing these effects.

5.2.1. Variation of irradiation time

In this paragraph results of experiments are presented for samples irradiated in OCP-mode during phase 3. The same experimental procedure as described in 5.2 was used, only the duration of irradiation in phase 3 was varied. All samples were taken from one production batch. Figure 23 shows the effects of varying the irradiation time.

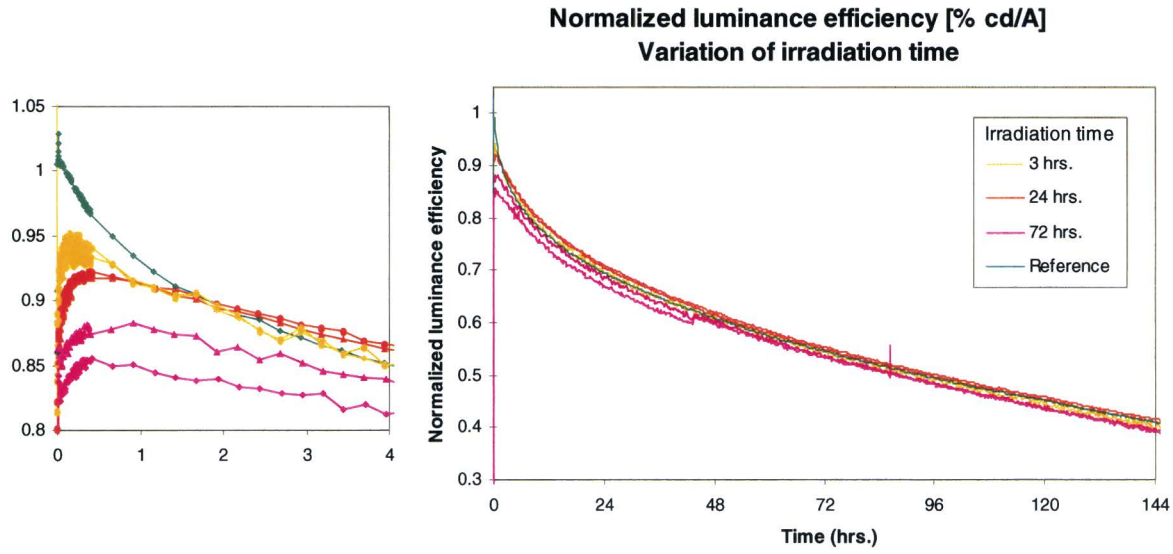

(a) *(b)*

Figure 23: Normalized luminance efficiency versus time (b) at constant electrical stress after different hours of irradiation at OCP. The different colours correspond to different irradiation times. In (a) only the first four hours of (b) are plotted and next to the vertical axis in colour the irradiation times are written for clarity. The initial (directly after irradiation) luminance values of the irradiated samples are up to 15% lower compared to the non-irradiated samples.

The right figure (b) shows the normalized luminance efficiency lifetime curve at constant electrical stress after different hours of irradiation at OCP. The green line always represents non-irradiated reference samples and is to be compared to irradiated samples. The figure shows that the 50% lifetime values from all the samples are almost identical, considering 100% as the value measured in phase 2, i.e. before irradiation. They have not changed significantly compared to the reference value. Some are slightly lower but others are even slightly higher.

The left figure (a) shows the same curves as (b), only for a different time scale, as indicated with the grey box in (b). First of all, the irradiated samples show an initial negative offset compared to the reference signal, decreasing with irradiation time. Secondly, the green tinted reference samples have an almost identical behaviour and on the long term also coincide with the irradiated samples.

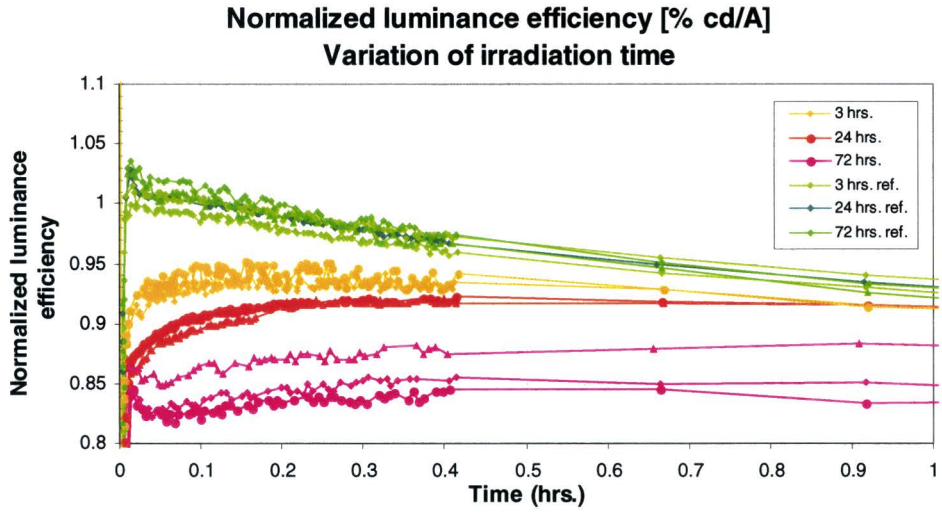

Figure 24: Normalized luminance efficiency curves (same data as in figure 23) during the first hour of operation at constant electrical stress after different hours of irradiation at OCP in comparison with non-irradiated reference samples indicating the reduced initial drop and therefore improved stability. Due to practical reasons, in the first 0.4 hours many data points were recorded.

Figure 24 shows only the first hour of the data from figure 23. During the first tens of minutes clearly a change of slope can be seen as function of irradiation time. Irradiated samples show a flattened slope in the first hour of operation and therefore improved stability compared to reference samples. Care has to be taken in interpreting data before 0.1 hours due to practical start-up effects, like overshoot and initial burn in.

Apart from normalizing to a characteristic value before irradiation occurred, there is also another approach in studying the effects of irradiation. If we regard external irradiation of a display as the last stage of the production process the effects are interesting for end-user display applications. The changed initial behaviour is what an end user would experience in an application, i.e. improved initial stability. In figure 25 normalized luminance efficiency lifetime curves are shown, however here the curves were normalized to data from after irradiation, i.e. data from phase 4, instead to the usual data from before irradiation, i.e. data measured in phase 2.

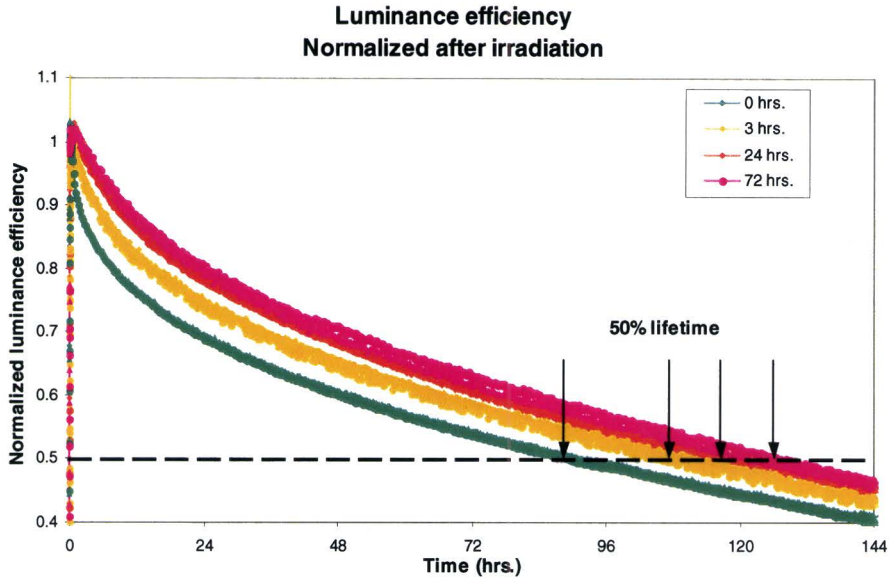

Figure 25: Luminance efficiency curves at constant electrical stress after different hours of irradiation (yellow, orange, purple) at OCP in comparison with non-irradiated reference samples (green) showing an increase of the 50% lifetime value. The curves are normalized on the usual way, only to data from after irradiation (phase 4), instead of before irradiation (phase 2).

Characterisation of the samples still occurred at the same current density (27.8mA/cm²) as always. The normalized luminance efficiency lifetime curves clearly show that the 50% lifetime value of a blue PolyLED can be improved by irradiating previously to operating.

This dependence of 50% lifetime value versus irradiation time is shown in by the red data points in figure 26 for several samples. In green and blue the data is represented from similar experiments with other production batches, but in their cases also a small amount of irradiation below 435nm, i.e. within the absorption band, occurred. Therefore care has to be taken when comparing the actual 50% lifetime values. The dotted lines do not represent actual data or a model, they are simply drawn to guide the eye through the data points.

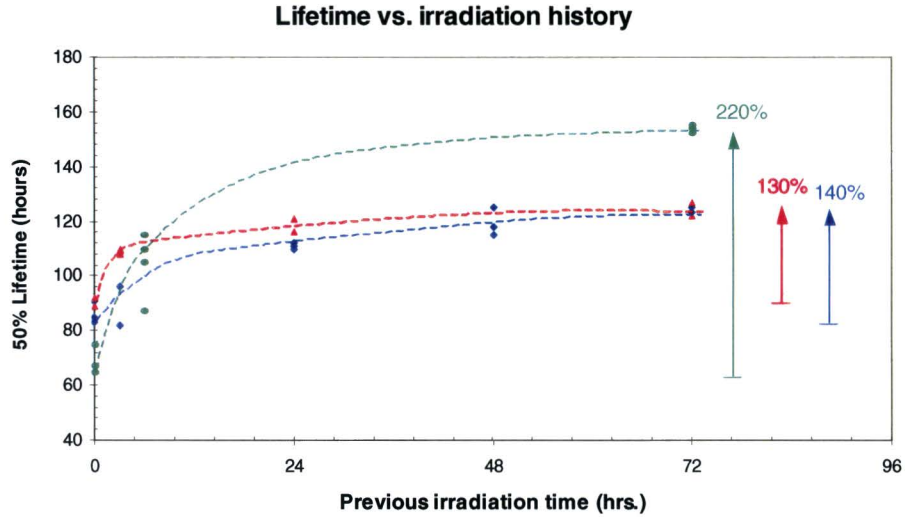

Figure 26: Lifetime values versus irradiation time. Lifetime values were taken from normalized luminance efficiency curves. Normalization was done after irradiation (like figure 25). The three colours represent data from similar experiments with three different production batches, however the experiments with green and blue data were performed before special covers (as mentioned in section 3.3) were made and therefore these samples were also irradiated with small amounts of light with wavelengths smaller than 435 nm, i.e. within the absorption band of the blue LEP. Each data point represents a different PolyLED sample. Next to the curves the lifetime increase is shown.

So, a trend in lifetime improvement due to irradiation is observed. Short term irradiation already has a significant effect, whereas many hours of irradiation leads to a saturation or plateau in the plot of 50% lifetime vs. irradiation history. In the experiments performed, this resulted in up to a factor 2 in lifetime improvement.

Apart from changes in optical characteristics shown so far, also electrical characteristics do change due to irradiation at OCP. Voltage and luminance are monitored simultaneously. The behaviour of voltage over time is illustrated in figure 27.

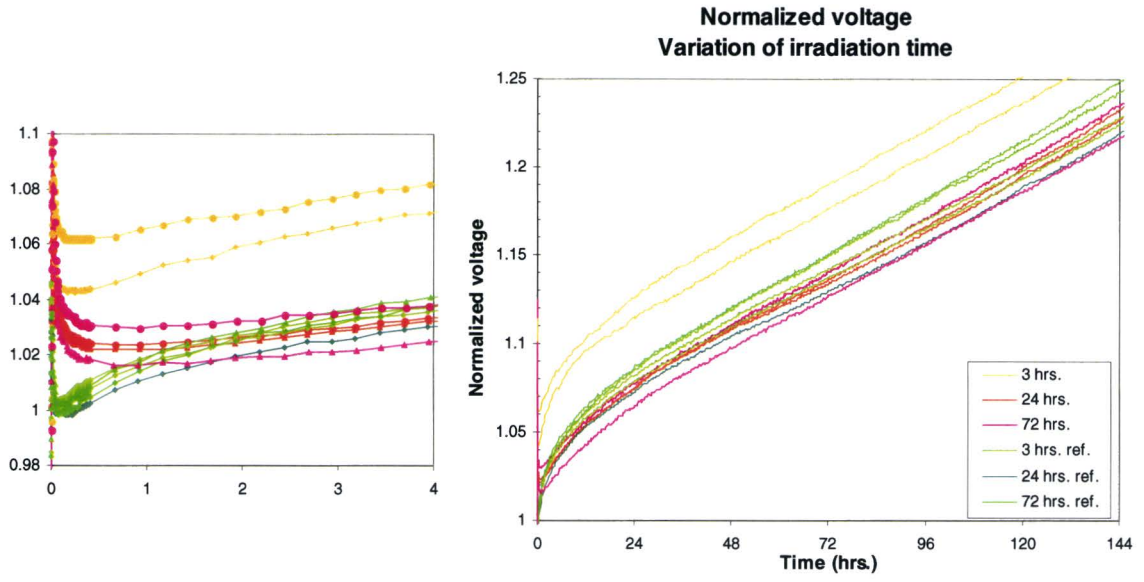

(a) *(b)*

Figure 27: Normalized voltage versus time (b) at constant electrical stress after different hours of irradiation at OCP. The different colours correspond to different irradiation times. The data correspond to figure 23, as luminance and voltage are recorded simultaneously. In (a) only the first four hours of (b) are plotted. A difference in initial offset and short term behaviour is observed.

As with the optical characteristics (illustrated in figure 23) again two effects are observed in the first few hours of operation: An initial offset and a change of slope, interpreted by an improved stability. On the long term the slopes are rather similar. The differences in initial offset can be caused by irradiation, but may also be due to bad electrical connections when samples are reconnected in the sample-holders after transferring them from the suntest set-up (phase 3, irradiation) to the lifetime set-up (phase 4, characterization). The contribution of these two could not be separated easily and therefore interpreting the voltage lifetime curves becomes more complicated than interpreting the luminance efficiency lifetime curves, which do not suffer from additional electrical contact effects as the current density is simply set to a fixed value. However, a change in behaviour, recognized as a change of slope, of the voltage lifetime curve apart from the initial offset is addressed to be caused by irradiation, since a bad electrical contact is considered to be constant over time.

This brings us to another way of looking at voltage lifetime curves. Instead of normalizing, vertically shifting the initial voltage value to, for example the value of a reference sample, cancels out all offset effects but helps comparing changes in behaviour, as illustrated in figure 28.

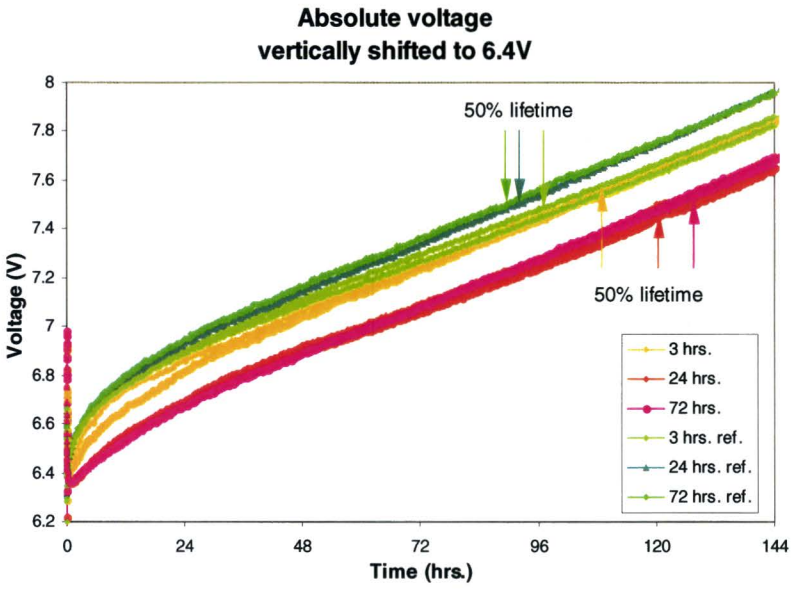

Figure 28: Voltage versus time at constant electrical stress after different hours of irradiation at OCP. The different colours correspond to different irradiation times. Irradiated devices show a mitigated voltage increase compared with their non-irradiated reference devices

It is clearly seen that the voltage increase is diminished by increased irradiation, which is wished from an applicational point of view. Creating an overview like figure 28 of the absolute voltage change during lifetime is also useful for studying the properties of PolyLEDs. Apart from the general focus in PolyLED research, i.e. trying to achieve longer 50% lifetimes for PolyLEDs, also a boundary condition of voltage change less than 1V at 50% lifetime applies. From figure 28 it can be seen that the voltage increase at 50% lifetime is about 1.1V for all samples, however lifetimes for irradiated samples are longer and therefore for irradiated samples it takes longer before the 1V threshold is reached.

In order to get an idea about the causes of the shown behavioural changes, the electro-luminescence (EL) and photo-luminescence (PL) spectra were studied of irradiated and non-irradiated samples. No spectral changes were seen in EL or PL between a sample directly after 72 hours of irradiation and a reference sample or even a virgin sample.

So far the results shown in this paragraph originate from one production batch. Qualitatively all the results reported in this chapter could be confirmed with samples of two other production batches.

5.2.2. Variation of electrical state

So far the reported results of irradiation regarded experiments performed at open circuit potential (OCP) whilst irradiating. However, one of the main research questions is whether degradation is an effect of interactions of photons alone or together with for instance charge carriers, excitons or trapped states. Irradiating samples kept at a different electrical stress, could give us more insight in the degradation processes involved that lie behind the effects shown in the previous paragraph (5.2.1).

In addition to OCP, two electrical stress states were of special interest, being irradiation at the built-in voltage and irradiation at a constant forward current. Applying the built-in voltage, i.e. 2.35V for the samples used here, onto a sample creates a net zero electrical field by cancelling the internal field between anode and cathode. At forward bias a positive field is generated

between the electrodes and in contrast to OCP and built-in, also several kinds of excited states and charge carriers are present in the LEP and off course the PolyLED is producing light by itself.

The experimental procedures corresponding to the results shown in this paragraph are similar to those described in the previous paragraph (5.2.1). The only difference lies in the fact that now in phase 3 samples were electronically connected and operated at constant electrical stress during irradiation. This also made monitoring the voltage during irradiation possible. The dedicated suntester set-up was specifically adapted to enable type of experiments. Of course the luminance of samples could not be measured inside the irradiation chamber.

The results shown in figure 29 involved an experiment of 72 hours of irradiation at constant electrical stress and at maximum power of the suntester. All experimental samples were covered with a 435nm cut-off filter, all reference samples were operated under dark conditions. There were four types of applied electrical stress: OCP (purple data), Built-in (2.35V, blue data), high Forward bias (27.8mA/cm², red data) and low Forward bias (0.56mA/cm², orange data). The corresponding reference samples are plotted in green tints. The high forward bias is identical to the current density used in phase 4 for characterisation after irradiation, which results in a roughly 50% degradation within about 90 hours.

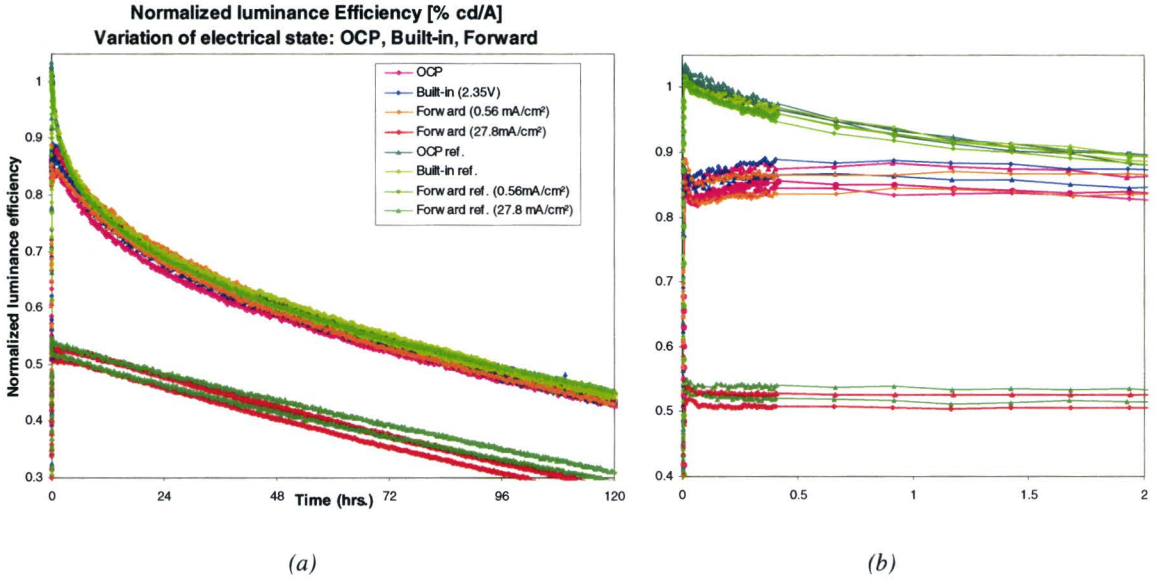

Figure 29: Normalized luminance efficiency versus time (a) operated at constant current after irradiation. The response was normalized to the corresponding value of pre-characterizing in phase 2. Samples were subjected to different modes of electrical stress during irradiation (referring to purple, blue, orange and red data points). In green tints the corresponding reference samples, i.e. subjected to the same electrical stress but not irradiated, are plotted. In (b) only the first 2 hours of operation after irradiation are plotted to show the initial behaviours.

Both on the long and short term, the behaviour of OCP-samples, Built-in-samples and low-Forward-samples is very similar, at least not distinguishable due to signal spread of similar samples. Their corresponding reference samples also behave similar. It can be concluded that photo-degradation is not directly linked to charge carriers or the presence of excited states.

The samples with high forward bias do show different behaviour compared to samples with low forward bias. In the figures their data points appear lower on the vertical axis but this is due to the fact that by stressing them for 72 hours they have already degraded, in accordance with expectations from the regular degradation curve as was shown earlier in figure 20. However,

samples stressed with a constant high forward bias show less initial offset compared to their corresponding reference samples after irradiation. They do not show an improved stability in luminance efficiency. Actually, their behaviour is similar to their reference samples. So for these samples only regular degradation is observed and no additional effects due to irradiation. The effects seen of photo-degradation relate to initial offset and initial stability. The change of slope of the red data in figure 29 compared to the corresponding green reference data (which becomes visible after about 24 hours of operation) might indicate a change in a degradation process on the long term due to photo-degradation but could also be considered normal behaviour since also reference samples normally do show a change of slope on that timescale (as was seen in figure 20).

In these experiments irradiation and electrical stress lasted for 72 hours, for similar experiments with shorter irradiation and stress times the effects due to irradiation were qualitatively similar. Only for the samples with high Forward bias the effects of initial offset and stability were slightly larger than shown in figure 29. Furthermore, care has to be taken in interpretation of the high Forward data, since the device produces large amounts of photons itself. It is estimated that the radiance power at high Forward is in the order of 10mW (the calculation is done in Appendix B), whereas the incident irradiation power is about 6mW. Therefore the contribution of the additional light source from the suntest set-up might be too small compared to the own light production by the device at high Forward bias. However, if photo-degradation is the dominant degradation process, the contribution of additional light should have been measurable and permanent.

It is concluded that the overall degradation in device performance is not mainly due to photons. It seems that electrical stress (electrical degradation) is the driving force in the degradation mechanisms and that photo-degradation plays a minor and certainly different role.

Voltage characteristics

So far the voltage characteristics were not mentioned in this paragraph. They were analyzed like the luminance efficiency curves and showed corresponding effects, supporting the conclusions. However, adaptations were made in the set-up for this study as described in the section 3.3 allowing us for the first time to monitor the voltage characteristics of a PolyLED whilst it was irradiated during phase 3. The results are presented here.

Figure 30 shows part of the voltage lifetime curve of a sample that was monitored during irradiation in the suntest set-up. Only two curves are shown for clarity representing the typical behaviour. The green curve corresponds to a non-irradiated reference sample at room temperature. The red curve corresponds to a sample that was operated for about 72 hours (in phase 3) with a current density of 27.8mA/cm^2 and was simultaneously irradiated for 72 hours in the suntest set-up. After that the irradiated sample was taken out of the suntest set-up and transferred to the standard lifetime set-up. There it was connected again and operated with a current density of 27.8mA/cm^2 (data beyond the t=74 hour mark). The reference sample was operated in dark, electrically identical including all hold times for sample transfer.

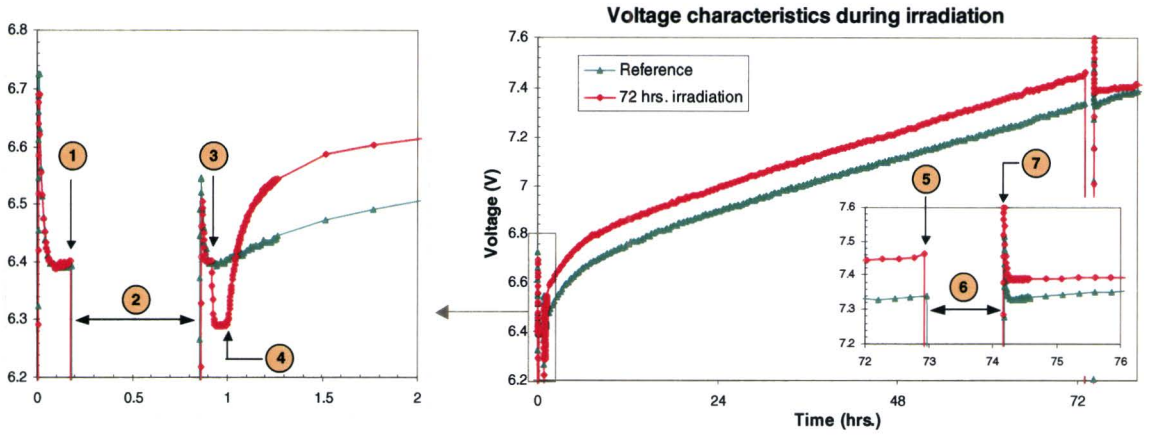

(a) *(b)*

Figure 30: Voltage versus time at constant electrical stress during simultaneous irradiation (between t=0.9 and t=72.9 hours) and after (t>74 hours). The first two hours are shown in (a), the behaviour on the long term is shown in (b). The inlet in (b) shows in detail the initial response of operation after irradiation. The red and green data corresponds to the typical behaviour of irradiated and (non-irradiated) reference samples, respectively. The numbers refer to change in treatment and are explained in the text below, during period (2) and (6) no electrical stress was applied. A swift response in voltage to temperature changes (between t=0.9 and t=1.3 hours) of the PolylED is observed as well as the typical initial offset after irradiation (at t>74 hours).

Figure 30 will now be explained in more detail. Initially (1) the green and red curve coincide, this is during pre-characterization (phase 2) in the first 0.2 hours. Then (2) all samples were turned off and samples represented by red data points were transferred into the suntest set-up. At the end of period (2) all samples were electrically reconnected and turned on again. This marks the beginning of phase 3. Two events mark the typical voltage response in the suntester from that point on. The first (3) is when the Xe-lamp of the suntester is ignited. This leads to a sudden temperature rise due to the infrared radiation of about 10°C which causes an immediate decrease in voltage. Next (4), about five minutes later, the Sun-Cool air-conditioning unit is automatically started, cooling the samples with air of about 15°C. Again the voltage responds rapidly to this temperature change. At about 20 minutes after ignition of the Xe-lamp (at about t=1.3 hours), the temperature in the suntest set-up reaches a steady state and the sample temperature is about 19°C. At t=73 hours the Xe-lamp was switched off (5) and samples were also turned off. The samples represented by red data points were transferred back into the standard lifetime set-up (6) and electrically reconnected. At t=74 hours (7) all samples were started again under dark conditions and identical temperatures, i.e. 20±2 °C. This marks the beginning of phase 4. The green curve resumes at about the same voltage. The red curve shows the meanwhile familiar initial offset due to irradiation. The initial value (7) is also slightly lower than the value at the end of irradiation (5). This is likely due to a warming up of the sample, back to room temperature.

From analyzing the voltage characteristics it is clear that the electrical properties are temperature dependent. Since the red curve rises slightly above the green curve due to the cooling (4) of the air-conditioning, it is concluded that the temperature in the irradiated pixel itself is lower compared to the reference sample. The actual real temperature of the LEP layer within a pixel can only be approximated by the temperature sensors. From reports about the voltage vs. temperature characteristics it is estimated that the temperature compared to the reference sample is about 4±1K lower [16].

From all the above results in this paragraph and those of identical experiments with irradiation times of 3 hours and 24 hours, which are not shown here, it can be concluded that irradiation with wavelengths larger than 435nm does influence the performance of a PolyLED. Photo-degradation becomes recognizable best in the cases whilst during irradiation no, or only a small, forward bias was applied and are recognizable as initial offset, initial stability improvement and 50% lifetime improvement, as can be concluded from this section and section 5.2.1. From the electrical state variation experiments it became clear that degradation effects due to electrical stress are much more dominant than effects due to irradiation.

5.2.3. Variation of wavelength regime

So far all experiments were done using a 435nm cut-off filter (Schott GG435) for each sample. In order to get a better idea what part of the light's spectrum is responsible for the effects seen so far, experiments were performed with different cut-off filters, corresponding to different wavelength regimes. The transmission spectra of the used filters are shown in figure 31.

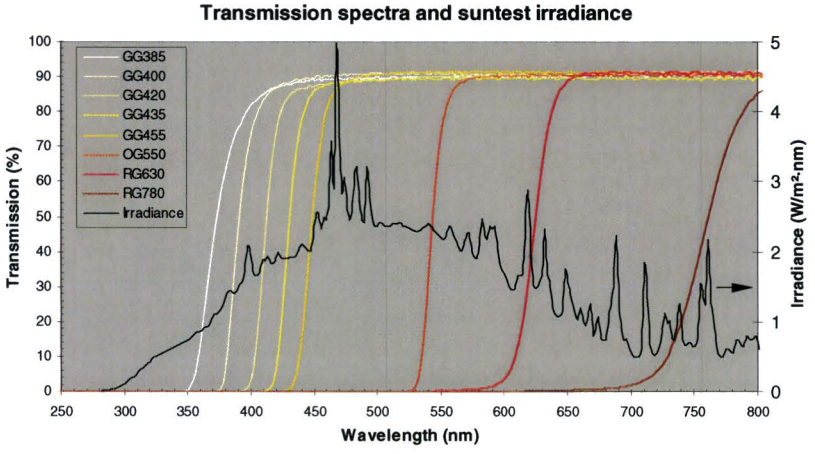

Figure 31: Transmission spectra of several used cut-off filters (left axis) and spectral distribution of the suntest Xe-lamp (right axis). By using a filter part of the spectrum of the Xe-lamp can be filtered away.

From the transmission spectra it becomes clear that all infrared radiation produced by the Xe-lamp is not filtered out and also might interact with the PolyLED. It will be shown that this does not influence the performance. Although the transmission of all used filters above the cut-off wavelength is similar, i.e. about 91%, when comparing the effects due to different wavelength regimes, quantitative analysis is not straightforward since the spectral power distribution of the lamp in the suntester is not uniform. However, these experiments are presented here as they contribute to the understanding of the effects of different photon energies on lifetime, initial offset and initial stability.

The experimental procedures corresponding to the results shown in this paragraph are similar to those described in the paragraph 1.2.1. In these experiments, all samples were irradiated for 72 hours at OCP and maximum power of the suntester, i.e. 765W/m² between 300nm and 800nm. All experimental samples were covered with different cut-off filters, all reference samples were kept under dark conditions. Samples were taken from one production batch only.

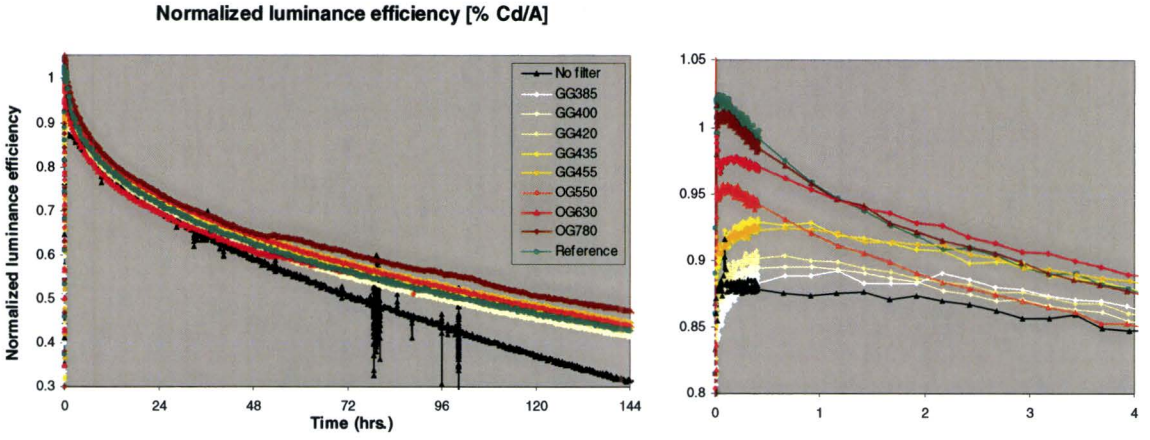

Figure 32: Normalized luminance efficiency versus time (a) operated at constant current after 72 hours of irradiation with different filters for each sample. In (b) only the first 4 hours of operation are shown. All lines represent the data from a typical sample (one chosen out of three) for reasons of clarity. The green line represents a non-irradiated reference sample. The black line represents a sample irradiated without any additional filter (at about 84 hours some unknown spikes occurred). In the legend the filter code (as defined by Schott) used for the matching sample is shown and the numerical value corresponds to the cut-off wavelength in nanometres (as was illustrated in figure 31). Different long term behaviour of the sample without a filter (irradiated far into the absorption band) is observed as well as a gradual shift in initial offset as function of the used filter.

Figure 32 shows the normalized luminance efficiency lifetime curve at constant electrical stress after different hours of irradiation with different cut-off filters at OCP.

The irradiated samples with filters all behave similar on the long term. Unfortunately, in this experiment, an error occurred regarding the temperature control of the samples represented by the brown and red line (filter OG630 and OG780) after 48 hours, i.e. temperature was a few degrees higher than room temperature which directly translated to a slight change in the measured characteristics. It is shown to demonstrate the observed trend and the effects on short term, since these effects have been reproduced by experiments with other production batches. The samples represented by the black line however do have changed lifetime characteristics on the long term, which becomes evident after about 40 hours of operation. Although no additional filter was used, the glass substrate of each PolyLED sample also acts as a cut-off filter ($\lambda > 325$nm). Nevertheless irradiation occurred far into the absorption band (as can be deduced from figure 17).

On the short term, as depicted in figure 32(b), a gradual shift in initial offset as function of the used filter is seen. Namely, irradiation with a broad spectrum (>385nm) leads to a large negative initial offset, whereas a smaller spectrum (>780nm) shows only minor or no initial offset. The same applies to the stability (here the slope of the response is a good measure for that) in the first few hours, i.e. an almost constant luminance efficiency behaviour for samples irradiated with a broad spectrum compared to a decreasing luminance efficiency for samples irradiated with a smaller spectrum.

Similar behaviour can be observed from the corresponding normalized voltage characteristics, as shown in figure 33.

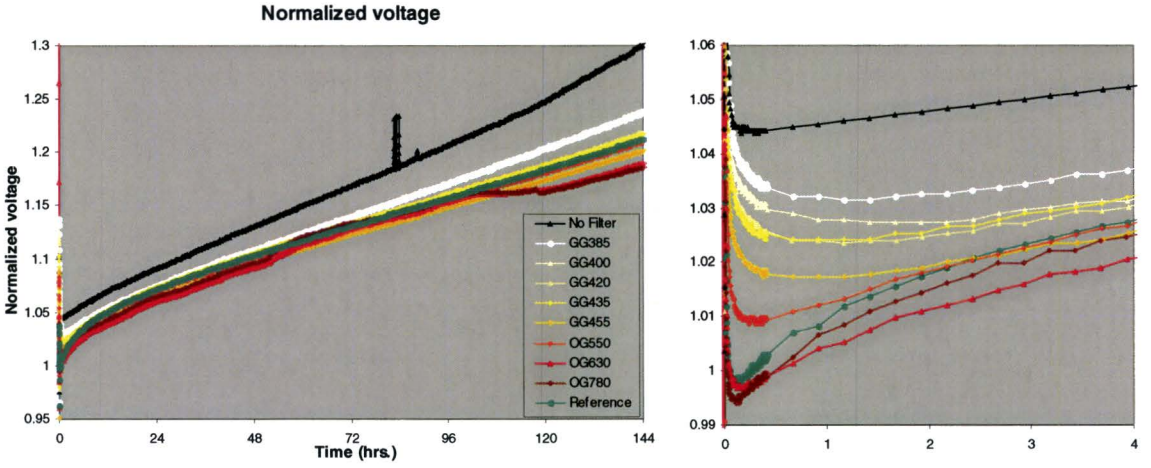

Figure 33: Normalized voltage versus time (a) at constant electrical stress after 72 hours of irradiation at OCP with a different filter for each sample. In (b) only the first hour of operation is shown. All lines represent the data from a typical sample for reasons of clarity. The green line represents a non-irradiated reference sample. The black line represents a sample irradiated without an additional filter (at about 84 hours some unknown spike occurred). In the legend the filter code (as defined by Schott) used for the matching sample is shown and the numerical value corresponds to the cut-off wavelength in nanometres (shown in figure 31). Different long term behaviour of the sample without a filter (irradiated far into the absorption band) is observed as well as a gradual shift in initial offset and stability as function of the used filter.

As with the luminance efficiency characteristics samples represented by the black line (no additional filter) show a clearly changed lifetime characteristic compared to reference samples. Otherwise both on the short and long term the effects described at the luminance efficiency are supported, i.e. on the short term gradual shift in initial offset and stability and on the long term similar behaviour. For a more quantitative analysis care has to be taken, since bad electrical contacts could result in an additional vertical shift in (b).

An important result from both figure 32 and figure 33 is that irradiation with infrared light ($\lambda >$ 780nm) shows no or hardly any effects compared to reference samples. The importance of this reflects also on the results discussed in paragraph 5.2.1, so that now can be concluded that only visible light (or UV-light) can be accounted for the effects of photo-degradation in the blue PolyLED, at least for the used irradiation intensities. From figure 32 (b) and figure 33 (b) it can be suggested that the initial offset is caused by different photon energies. However, quantitative interpretation of the observed changes is not that simple and straightforward since, due to the different filters and the non-uniform spectral radiance of the lamp, samples received different amounts of light dose during the 72 hours of irradiation. For example, when using the GG400 filter a sample was irradiated at about 6mW (400nm-800nm), and when using OG630 at about 1.5mW (630nm-800nm). In section 5.3.1 it will be shown that higher intensities for wavelengths around 650 nm still result in a smaller initial offset or luminance efficiency loss. Also in section 5.3.1 another problem, i.e. the spread in signals from similar samples (which is not shown in figure 32 for reasons of clarity) will be taken care of. This will make comparing and interpreting the effects due to photon energy less complicated.

The experiments in the suntest set-up using cut-off filters showed already some clear qualitative trends. Since irradiation occurred over an integral part of the spectrum, the effects of particular wavelengths are difficult to accurately quantify. In order to make a more quantitative analysis possible a wavelength dispersed study is needed and will be presented in 5.3.

5.2.4. Reversibility and shelf effects

Now that we have seen some of the effects of light with regard to the PolyLED performance, the question to what matter these effects were lasting or annihilated over time became urgent.

To get a better idea about the reversibility (or lack of) an experiment similar to the one described in the previous paragraph 5.2.3 was performed. However, this time all three 3mm by 3mm pixels were pre-characterized in phase 2, then 72 hours of irradiation at OCP followed with different filters. The first of the three pixels was characterized in the lifetime set-up directly afterwards. The second pixel was stored at OCP and room temperature for 377 hours (15 days and 17 hours) and subsequently characterized. The third pixel was stored at OCP of which 409 hours at room temperature and the last 17 hours at 50°C for 426 hours (17 days and 18 hours) and subsequently characterized. The waiting times between phase 3 and phase 4 are referred to as additional shelf times. The normalized luminance efficiency responses are plotted in figure 34 and only the first four hours of operation are shown.

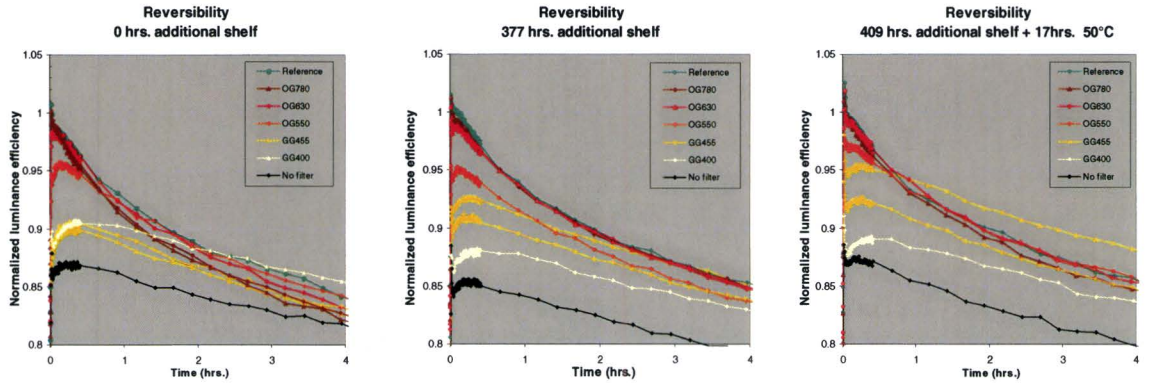

Figure 34: Normalized luminance efficiency curves at constant electrical stress after 72 hours of irradiation with different filters at OCP; (a) directly after; (b) after 377 hours of storage under dark conditions at room temperature and at OCP; (c) after 409 hours of storage at room temperature followed by 17 hours at 50°C, all under dark conditions and at OCP. For (a), (b) and (c) samples were irradiated once, only different pixels on the same sample were characterized successively. Only one curve is plotted for each filter for clarity. Two data-lines are plotted for samples using filter GG455 to illustrate sample to sample spread which is typical for all signals. The spread increase from (a) to (c) for GG455 is coincidental and does not apply to the other samples. The figures show a long lasting effect of initial offset for shelf conditions at room temperature. A slight effect of reversibility due to an elevated temperature results in a smaller initial offset for all samples.

In (a) we can recognize the characteristics described in section 5.2.3. After storing the samples 377 hours (b) there are no significant changes in characteristics recognizable. The differences that can be seen are regarded to be due to pixel to pixel variations within one sample. This is also supported by the sample to sample variations, illustrated by the spread in signal when plotting the data from a second sample, e.g. GG455 in each plot. Comparing (c) to (b) then, a slight reversibility effect can be observed, resulting in a smaller initial offset for all samples. This might be caused by the higher storage temperature of 50°C compared to room temperature. Higher temperatures were not tested, since in that case also shelf effects for non-irradiated samples occur which is out of the scope of this study.

Overall from these experiments it can be concluded that the loss in initial luminance efficiency is conserved over time, at least for the observed 18 days. Shelf effects due to simple storage of samples under dark conditions at room temperature and OCP were not measurable. Figure 34 already showed this on a short term. Experiments to measure shelf effects at virgin samples over

several months did not show characteristic changes, not for the short term nor for the long term (50% lifetime values).

5.3. Wavelength effects

From the suntest experiments with filters it became obvious that light outside the absorption band of the LEP influenced the performance of a PolyLED, although this was against expectations. Interaction of the LEP with light within the absorption band could be expected due to creation of excited states. In order to get a better understanding what part of the visible spectrum is involved in photo-degradation the Rainbow set-up (as explained in section 3.4) was built as an alternative to the wavelength study with filters used in the suntest set-up. With this Rainbow set-up a wavelength disperse analysis of the photo-degradation effects directly after irradiation becomes possible. Combined with the results of lifetime studies performed with the suntest set-up, both of them provide a more comprehensive understanding of the effects of photo-degradation.

There are several advantages: 1) the effects of all wavelengths can be measured simultaneously in one device as function of position within the rainbow, therefore there is no signal spread due to sample variations; 2) spectral resolution is improved compared to using a limited amount of filters; 3) no spikes are present in the spectrum of the light source and nor any possible infrared interactions. Off course there were also some disadvantages and challenges which will be explained and partially solved when showing the results in the next paragraphs.

5.3.1. Rainbow greyscale analysis

In the rainbow set-up individual samples were irradiated separately. Unless mentioned otherwise, the large #1 pixel of a sample was used for experiments. A bias of 10mA (corresponding to a current density of 1.74 mA/cm^2) was applied to a sample for several seconds and with the help of the CCD-camera a picture of the electroluminescence was taken to check the homogeneity of the pixel. Selection of a sample for the experiment was done on the basis of the absence of dark or light spots, spin coating stripes and spin coating irregularities due to dust particles. This resulted in homogeneous samples for experimentation with less than 8% overall deviation in EL intensity (apart from boundary effects), and less than 3% deviation in EL intensity in the area selected to be irradiated.

After selecting a suitable sample, it was placed in the rainbow set-up for irradiation. First a part of the pixel was irradiated using an interference filter (Schott BG35) at an intensity of about 1 mW (integral over the full rainbow). This lasted typically between 24 hours and 72 hours and the sample was kept at open circuit potential (OCP). Already after several hours of irradiation effects became visible in the electroluminescence of the pixel, but for a better resolution and signal to noise ratio longer times were preferred. Subsequently the sample was vertically shifted and a non-irradiated part of the pixel was irradiated using a 400nm cut-off filter (Schott GG400) for the actual experiment. For this second part of the experiment a new lamp for the light source was used (because of the limited lifetime of the lamp) and irradiation occurred for 72 hours at OCP. This irradiation corresponds to phase 3 as used in the experimental procedures for the suntest set-up. After irradiation the sample was placed in front of the CCD-camera and images were taken of the electroluminescence (EL) with a bias of 10mA (current density of 1.74 mA/cm^2) and the photoluminescence (PL) using a UV lamp. Comparing to the samples irradiated in the suntest set-up, the state of the sample when the image was taken corresponds roughly to the first set of data points of phase 4.

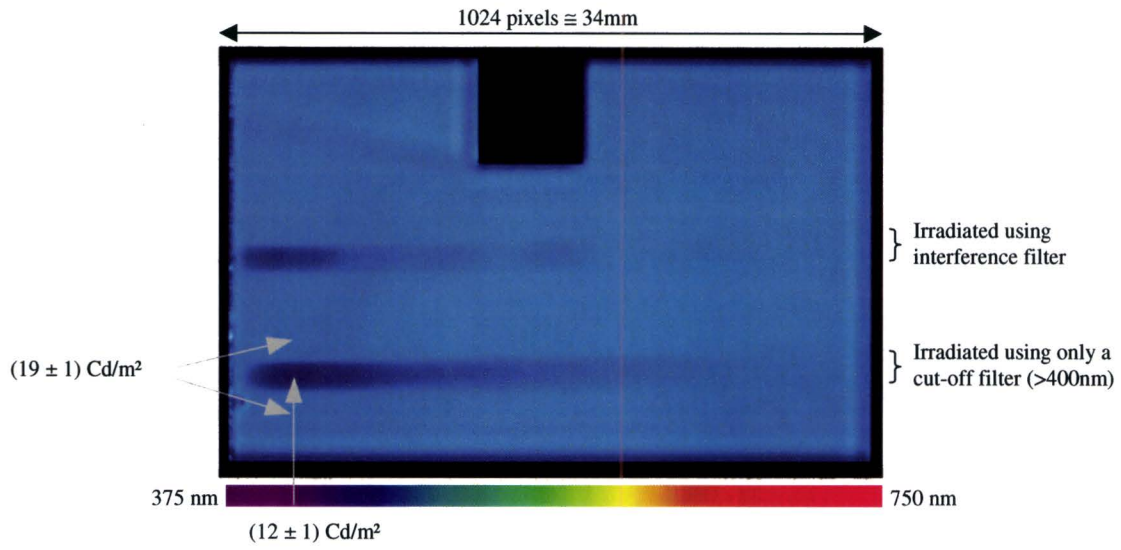

Figure 35: Photo of a large pixel irradiated twice with a rainbow spectrum of visible light: the upper dark strip was irradiated using an interference filter to calibrate the wavelength axis, the lower dark strip was irradiated with the full spectrum using a cut-off filter (>400nm) with blue on the left and red light irradiation on the right hand side. A loss of luminance as function of wavelength is observed. To quantify the loss of luminance, the lowest value (12 cd/m²) in the lower irradiated strip and a typical value (19 cd/m²) for the surrounding non-irradiated reference region are shown.

In figure 35 a photographic image of the EL of pixel #1 is shown, demonstrating the loss in luminance as function of position. The upper strip is irradiated using an interference filter to pin a wavelength to each of the 1024 horizontal pixels of the photographic image. The lower strip is irradiated with the full visible spectrum using a cut-off filter to make sure no UV light from a higher order irradiates the device. Underneath the photographic image of figure 35 the visible spectrum illustrates at what position approximately what colour was incident.

Apart from the conversion of position to wavelength, the upper strip is also used to verify the spectral resolution of the optical system. A good resolution (minimized overlapping of neighbouring wavelengths) is important for the interpretation of the results. In figure 36 a line profile (explained in 4.4.1) through the upper strip, represented in red, is compared with the transmission spectrum, plotted in blue, of the interference filter used for calibration of the wavelength scale.

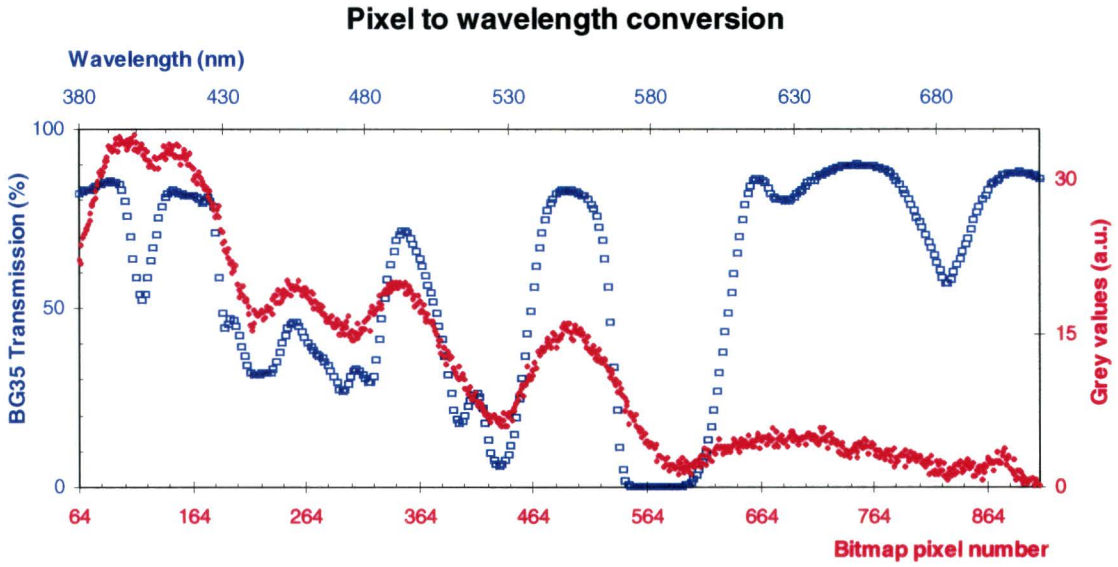

Figure 36: Grey values of a line profile scan through an irradiated strip vs. location on the pixel (red, right axis) compared to the transmission spectrum (blue, left axis) of the used interference filter. Peaks in the blue data correspond to locations of higher irradiation intensity. The locations of the blue peaks are matched to the loss of luminance (grey value) peaks observed in the line profile scan.

In the line profile the luminance loss is obtained from the grey values measured by the CCD-camera. The higher the grey value, the larger the loss of luminance, i.e. the darker the strip in figure 35. A peak in the blue data corresponds to a higher transmission and thus a local intensity maximum of irradiance on the sample. Assuming that a localized peak in intensity causes a localized loss in luminance, all recognizable maxima and minima in figure 36 can be matched. By a best linear fit through the gathered data points, an expression to convert pixel value to wavelength value is obtained. The heights of different red peaks do not correspond to the heights of the matching blue peaks. Clearly light from the blue end of the visible spectrum causes more loss of luminance than light from the red end. This is understandable as we already know from the suntest experiments in section 5.2.3 that the loss in luminance efficiency of the PolyLED decreases with increasing wavelength. However, due to the spectral radiance of the lamp (as depicted in figure 10), the intensity of the incident blue light is much lower than that of the incident red light. So, from the downwardly trend of the red data in figure 36 it can be concluded that photons with smaller wavelengths contribute to more luminance loss than photons with larger wavelengths, at least in the visible spectrum. This was already suggested by the suntest experiments in section 5.2.3, but could not be fully concluded yet.

To obtain a dependence of luminance loss as function of photon wavelength or energy, we study the lower strip in figure 35 in more detail. First a line scan profile is made through the strip that was irradiated by the full spectrum (>400nm) of the halogen lamp. Since the spectrum of the lamp is not uniform, the grey values from the CCD-camera are adjusted for the spectral power distribution. The same is done for the non-uniform grating efficiency. In doing so we now have assumed a uniformly constant irradiance spectrum (between 400nm and 800nm). Furthermore wavelengths are converted into photon energies. Now the recalibrated grey values are normalized and plotted against photon energy in figure 37.

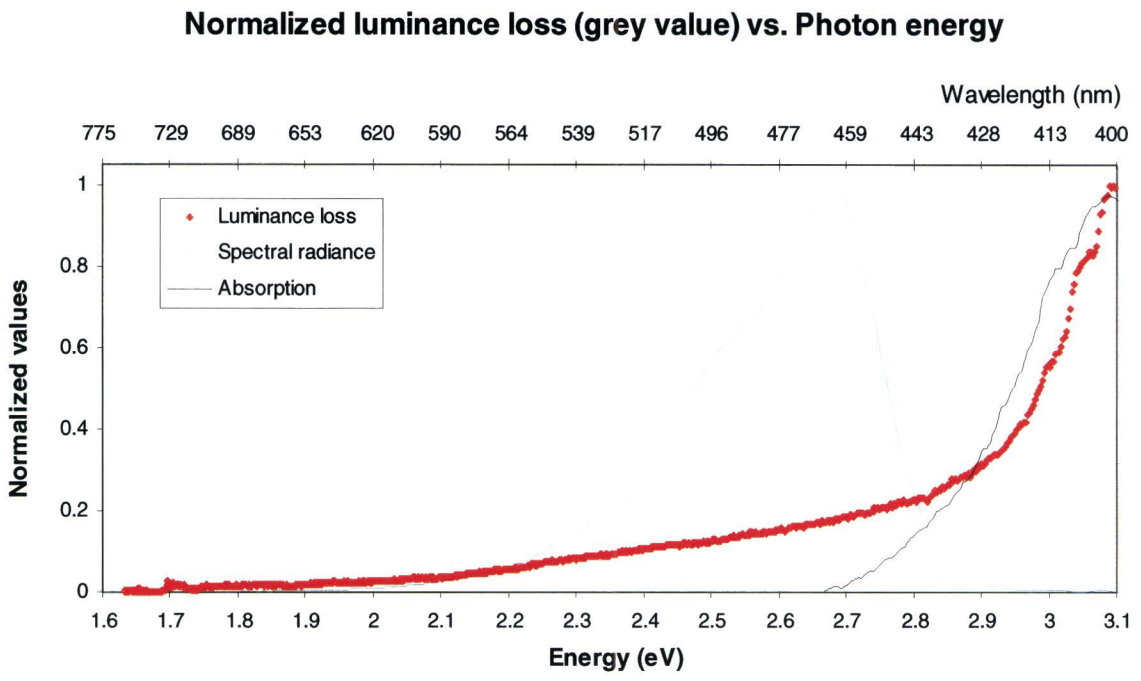

Figure 37: Normalized (to the largest grey value at 3.1eV=400nm) and recalibrated grey values (orange) versus photon energy of the irradiation source (the non-linear wavelength axis is indicated above the plot). An overall increase in grey value, regarded as luminance loss, is observed as function of photon energy. At about 2.8eV (≅450nm) a steep rise is observed. Also plotted in black and blue are, respectively, the absorption and the normalized spectral radiance of the LEP vs. photon energy. The steep rise matches the beginning of the absorption band, i.e. the energy at which excitons in the LEP are created. Light with wavelengths emitted by the LEP itself cause a considerable loss of luminance, even for wavelengths outside the absorption band.

The spectral radiance (blue) of the LEP and its absorption (black) are also plotted in figure 37 to identify the relevant energy regimes for interpreting the results. Luminance loss (orange data points) is lowest for low photon energies and increases slowly up to about 2.8eV. For higher photon energies the luminance loss increases rapidly. The energy of 2.7eV corresponds to the lower end of the absorption band. From this point on excitons are being created by absorption of the light and another degradation mechanism is activated which also contributes to a loss in luminance. Moreover, figure 37 shows clearly a considerable loss of luminance due to photons with energies lower than 2.7eV, i.e. outside the absorption band. This was not expected, since the photons outside the absorption band do not interact with the LEP, at least not in a direct way. Comparing this regime to the spectral radiance (blue) it becomes clear again that light with wavelengths corresponding to wavelengths emitted by the LEP itself contributes to degradation.

However, a physical interpretation of the grey values is not straightforward. Clearly a high grey value corresponds to a high loss in luminance. But this could be due to a loss in luminance efficiency (e.g. due to changed mobilities of charge carriers or due to deteriorated injection of charge carriers) or due to a redistribution of the local current density at the location of the partially irradiated pixel. In order to measure the current density as function of wavelength and to study in which way the luminance efficiency has changed yet another experiment was performed.

For this experiment a sample was placed in the rainbow set-up such that the three 1mm by 1mm pixels were fully irradiated. Irradiation occurred at the same conditions as with the sample the data in figure 35 and figure 37 originates from, i.e. 72 hours irradiated at OCP and $\lambda > 400$nm. Due to the dimensions of the small pixels and their relative positions this resulted in irradiation with blue light (415 ± 15 nm), green light (540 ± 15 nm) and red light (660 ± 15 nm). Before and

after irradiation current-voltage-luminance-curves (as introduced earlier, see for instance figure 18) were measured for each pixel. The same was done with a non-irradiated reference sample to rule out shelf effects. Due to pixel to pixel variations a slight spread in the IVL-curves was observed. Therefore IVL-curves of irradiated pixels were normalized to the IVL-curves measured before irradiation to compare and more easily interpret results. The normalized luminance efficiency curves for the three pixels are shown in figure 38.

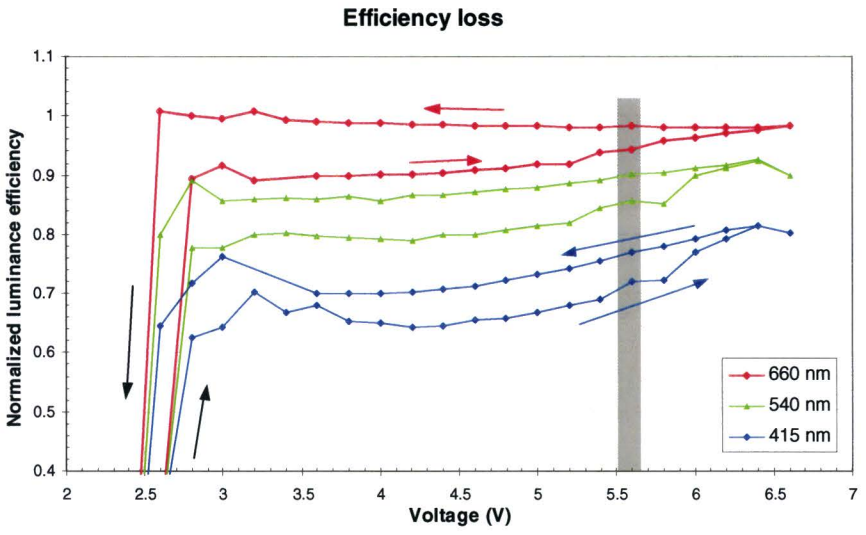

Figure 38: Normalized luminance efficiencies of three different pixels on one sample after irradiation with 415nm (blue, pixel 2), 540nm (green, pixel 3) and 660nm (red, pixel 4) versus applied voltage. Normalization was done with respect to the luminance efficiency curves of the same pixels before irradiation. Irradiance intensities were according to the spectral radiance of the lamp, meaning highest intensity for red, lower for green and lowest for blue. Nevertheless, the largest loss of efficiency is observed for blue. The arrows indicate the direction of the applied voltage sweep when measuring the IVL-characteristics. The grey area around 5.6V indicates the region of operation of the LEP in which the image in figure 35 was taken.

The three colours (red, green and blue) represent the three pixels irradiated with different parts of the visible spectrum. Voltage was swept from -2V up to 6.6V and back again. The voltage at which light is produced by the LEP, i.e. built-in voltage of 2.4V, has not changed due to irradiation. However, the luminance efficiency has changed for the different pixels due to irradiation, as is clearly seen in figure 38. For the pixel irradiated with wavelengths of about 660nm the efficiency loss is up to 10%, for the pixel irradiated with wavelengths of about 415nm it is between 20% and 35%. Moreover, each pixel was irradiated with a different intensity, due to the spectral radiance distribution of the light source (as illustrated in figure 10). The intensity was highest for red light and lowest for blue light. Therefore, the differences in luminance efficiencies for a uniform light source would be even larger than shown in figure 38.

From figure 38 a correct conversion for grey values measured by the CCD-camera to loss of luminance efficiency can be made. And the grey area around 5.6V in figure 38 corresponds to the electrical stress applied to a sample shown in figure 35. Relating these results back to figure 37 means that the grey values on the vertical axis can not only be considered as simply loss of luminance, but actually represent a loss of luminance efficiency.

It can also be seen in figure 38 that the loss in normalized luminance efficiency is not constant when increasing voltage. It might indicate that the applied electrical stress affects the reversibility effect already seen with photo-degradation in section 5.2.4. The observed hysteresis in each curve could also support that. Furthermore it is supported by the fact that consecutive voltage sweeps

show less loss in normalized luminance efficiency. The pixel represented in red comes to a full recovery after already one voltage sweep, the pixel represented by blue does not fully recover and shows a more permanent normalized luminance efficiency loss.

So far the results in this paragraph were gathered from EL images. Photoluminescence images were also analyzed but showed no measurable effects. This means that the bulk of the LEP is not affected by the photons, at least for the applied irradiation intensities. It also could mean that only a small part of the LEP is affected, e.g. at an interface, and that the PL of the rest of the bulk LEP overshadows a loss of signal. The reduced EL observed might therefore also be solely interface related. In section 5.4 this will be studied closer when samples were irradiated with lasers having much higher intensities than the light from the rainbow beam.

Reflecting the results of this paragraph back to the irradiation experiments in the suntest set-up (section 5.2.3) we have to keep in mind that the EL images shown here are taken shortly after irradiation. This is comparable to the data within the first few minutes of operation in phase 4 as shown e.g. in figure 32, which confirms at least qualitatively the loss of luminance as function of photon energy or wavelength. In order to check whether the initial offset in luminance efficiency also annihilates over time when compared to a reference signal, as was the case in the suntest experiments, a similar sample as shown in figure 35 was operated in forward mode with a current density of 1.74mA/cm^2. Within 2 hours the initially clearly recognizable dark strip vanished, i.e. was no longer distinguishable from the surrounding area in the pixel. Several hours later, slowly the part of the strip previously irradiated with the blue part of the visible spectrum became slightly brighter than its surrounding reference. So the contrast as seen in figure 35 inverted. This again is consistent with the behaviour of the normalized luminance efficiency characteristics on the long term as seen in the previous paragraphs of section 5.2. Due to lack of time and practical circumstances this was not further studied in detail with other samples.

5.4. Interface effects

From all the previous paragraphs in this chapter it became obvious that visible light affects the performance of the PolyLED. Although in the electroluminescence (EL) changes were observed after irradiation, this was not the case for the photoluminescence (PL), not even for light with wavelengths within the absorption band. Because of that it is not clear what part of the PolyLED is actually damaged by the light. Irradiation with a higher intensity was applied to investigate the PL results. On the other hand it also indicated that the bulk of the LEP layer may not be damaged directly but one or more of the interfaces or other layers in the device play a crucial role in the degradation process. [redacted] This would ultimately lead to a loss in luminance efficiency.

To check if the LEP-cathode interface is damaged by light, an experiment was set up to irradiate samples during production in the pre-pilot line at Philips Research to study irradiation effects before cathode deposition and directly after complete fabrication, i.e. with a cathode present during irradiation.

5.4.1. Irradiation with and without cathode

Goal of this irradiation experiment during sample fabrication was to prove if the LEP-cathode interface is damaged due to irradiation. Therefore samples were taken shortly out of the production process and irradiated inside a glove box for several minutes with a powerful green

(55mW, 532nm) and blue (12mW, 404nm) laser before the production step of cathode deposition.

In the regular production process, after spin coating the PEDOT layer and LEP layer samples are transferred into a nitrogen glove box with protected atmosphere (less than 1 ppm O_2, less than 1 ppm H_2O). From here samples normally are transferred into an evaporation chamber for cathode deposition, followed by encapsulating the device which ends the fabrication process. In our experiments samples were irradiated in the glove box environment before cathode deposition. Care was taken to minimize oxidation processes of the LEP by delaying the production process as little as possible, i.e. experiments lasted about 25 minutes. It is well known in production that this waiting period does not reduce device performance. Also the photo-luminescence of the LEP irradiated by the blue laser was monitored over time with a luminescence meter, which showed no changes.

Irradiation with the blue and green laser occurred simultaneously on different samples. The green laser irradiated the large pixel #1 for 2, 4 and 10 minutes at different positions. The blue laser irradiated the large pixel #1 of another sample for 2 and 20 minutes at different positions. Next, samples were transferred into the evaporation chamber for cathode deposition and final production processes. Directly after fabrication the EL and PL of the irradiated samples were measured. Samples irradiated with the green laser showed no changes in EL and PL. Samples irradiated with the blue laser did show small changes in EL and PL.

The second step of the experiment was to repeat the irradiation on the same device, but in the presence of the Ba/Al cathode, at open circuit potential (OCP). Different areas within the previously irradiated pixel were chosen for irradiation, to make effects easily comparable.

Figure 39 shows an image, taken with CCD-camera of the Rainbow set-up, of the EL of a sample irradiated with the green laser (55mW, 532nm).

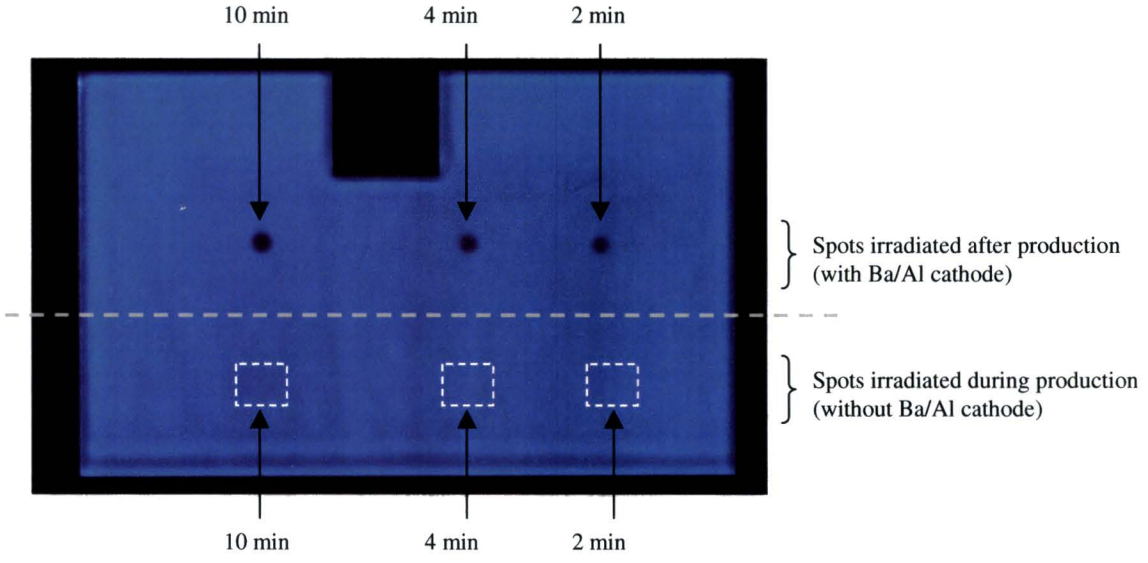

Figure 39: Photographic image of the electroluminescence of a large pixel in forward mode (current density 1.74mA/cm²) after irradiation of the same sample with a green 532nm, 55mW unexpanded laser beam before cathode deposition (lower half) and after cathode deposition (upper half). Irradiated areas are marked with arrows and corresponding irradiation times are indicated. The square boxes in the lower half indicate the area of irradiation before the cathode was presence, but show no changes.

Three distinctive irradiation spots in the upper part of the pixel are recognizable. They correspond to irradiation after production with the Ba/Al cathode present. The different

irradiation times are indicated. The lower part of the pixel was irradiated in the nitrogen glove box before cathode deposition and the locations of irradiation with the laser and the corresponding irradiation times are indicated, but no effects are observable. In PL no effects were observed at all. This clearly shows that degradation is induced due to the presence of the cathode although irradiation occurred with a 532nm laser, i.e. outside the absorption band.

A line scan profile of the luminance through the three spots in the upper part of figure 39 is shown in figure 40 for a more quantitative analysis.

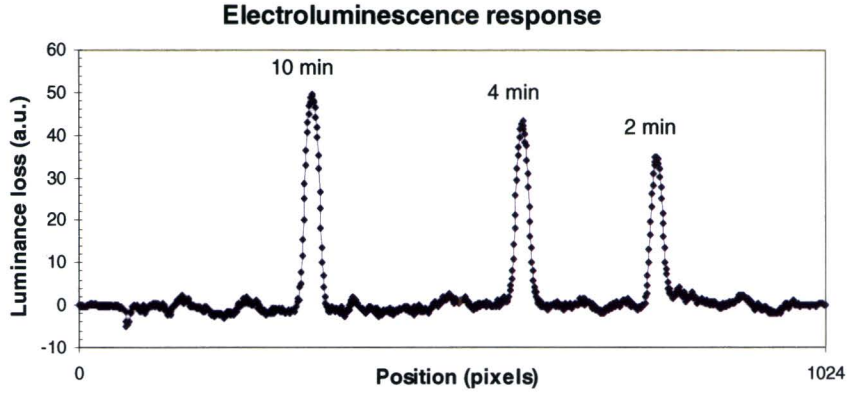

Figure 40: Line scan profile of the EL through the three distinctive irradiation spots as depicted in figure 39. Irradiation was done with a green (532nm) laser in the presence of the cathode.

The grey value (luminance loss) is plotted as function of position. The three irradiated spots are clearly recognizable. It can also be seen that the luminance loss is not linear with irradiation time. The data suggests a saturation of luminance loss. It also indicates that most photo-degradation occurs already in the first period of irradiation.

In PL, no change of signal on the irradiated spots was observed for the green laser. However, for the blue laser spot both the EL and the PL responses changed. This is shown for the EL in figure 41.

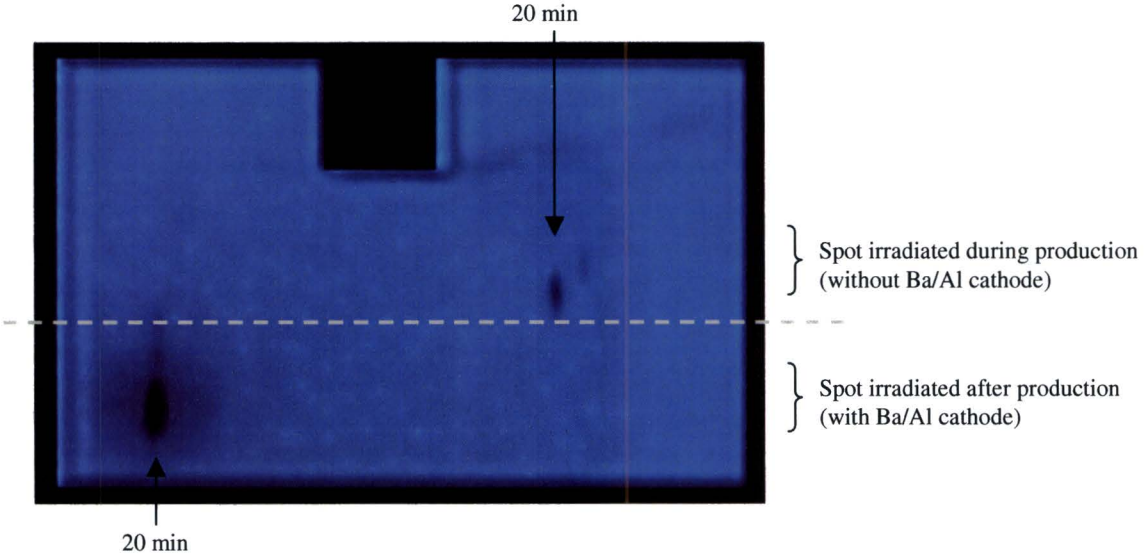

Figure 41: Photographic image of the electroluminescence of a large pixel in forward mode (current density 1.74mA/cm²) after 20 minutes of irradiation of the same sample with a 404nm laser before cathode deposition (lower half) and after cathode deposition (upper half). Irradiated areas are marked with arrows.

Again the spot irradiated in the presence of the cathode (bottom left in figure 41) is clearly visible. However, also the area irradiated without the cathode present (middle right in figure 41) can be distinguished. Since the wavelength of the blue laser (404nm) lies within the absorption of the LEP the loss of luminance is also assumed to be caused by excitons generated in the bulk, leading to a different degradation mechanism that applies (at least) to the bulk of the LEP. Due to the out-coupling of the blue laser its laser spot was different of shape and more spread out compared to the green laser.

Line scan profiles were made through the irradiated areas as depicted in figure 41 for both the EL and the PL responses and are shown in figure 42.

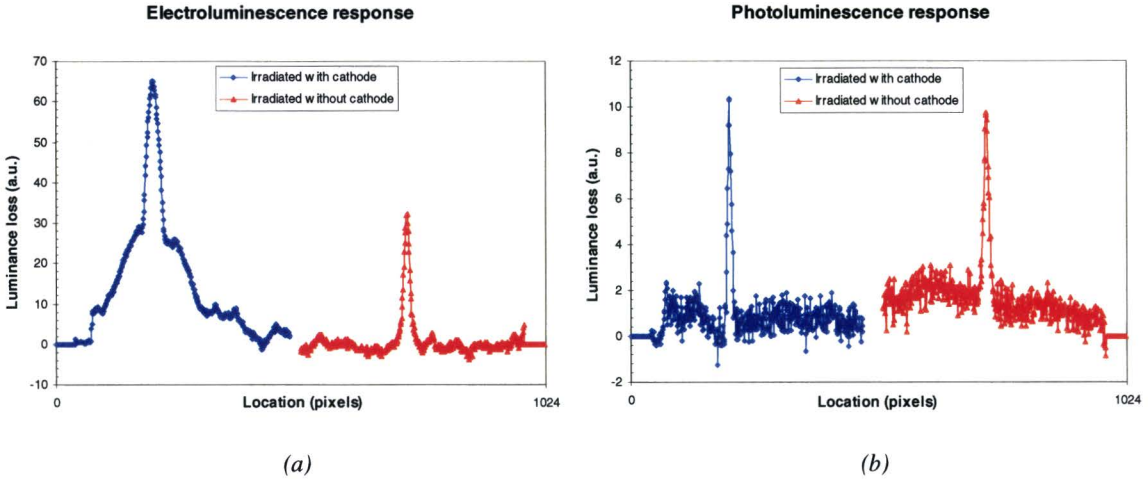

Figure 42: Line scan profile of the EL (a) and PL (b) through the distinctive irradiation spots as depicted in figure 41. The orange and blue data corresponds to irradiation with a blue (404nm) laser before and after cathode deposition, respectively.

In the electroluminescence response (a) clearly the differences in luminance loss can be seen. The shape of the blue curve resembles the intensity profile of the laser spot. Comparing the orange to the blue curve it can be seen from the shape of the curves that only the centre of the laser spot (intensity maximum of the unexpanded beam) is to be accounted for the bulk degradation, as there are no shoulders identifiable in the orange signal. This is also supported by the response from the PL (b), in which the curves are similar to each other (in height and shape) and the intensity profile of the blue laser cannot be recognized, i.e. only a sharp narrow peak is observed.

After the laser spot experiments all samples were stored under dark conditions at OCP. Two months later the effects in EL and PL were still present.

Comparing the results from irradiation with the green laser to irradiation with the blue laser, the following can be concluded. Since the intensity of the blue laser was lower than the intensity of the green one (12mW and 55mW respectively), but still the loss of luminance was higher for the area irradiated by the blue laser, this experiment confirms the conclusions as seen in section 5.3.1 (rainbow analysis), namely that light with higher photon energies contributes more to degradation than light with lower photon energies. It also shows that blue light (404nm, so within the absorption band of the LEP), contributes in the degradation of the bulk LEP, whereas this is not the case for green light (532nm, so outside the absorption band of the LEP and even higher irradiation intensity).

Furthermore, it is clear that the presence of the Ba/Al cathode provides a condition for light with wavelengths outside of the absorption band to contribute to photo-degradation.

Reflecting the results and conclusions back to the previous results from the suntest experiments (section 5.2) and the rainbow experiments (section 5.3), and keeping in mind that the images in figure 39 and figure 41 were taken shortly after irradiation, it can be concluded that laser-experiments do support the previous conclusions regarding photo-degradation as function of wavelength. The irradiated areas of figure 39 correspond to data from the first tens of minutes of operation after irradiation as characterized previously in the suntest experiments (section 5.2). After several hours of operation the luminance of an area irradiated with the green laser became comparable to the surrounding reference area, corresponding to the signals from the suntest experiments that became comparable in behaviour to their reference samples (as was illustrated in figure 32(b)).

6. Discussion

All the results presented in chapter 5 were obtained from experiments involving three different light sources (short-listed in table 1). Furthermore, an estimated calculation is presented for the order of radiation intensity inside the PolyLED, i.e. about 10mW/cm² (calculation is done in Appendix B: Estimation radiation power PolyLED).

Table 1: Overview of used irradiation sources compared to a PolyLED

Set-up / Light source	**Power (mW/cm²)**	**Range (nm)**	**Dose (kJ/cm²)**	**Remarks**
Suntest / Xe-lamp	17 - 67	400 - 800	0.7 - 17	Broad bandwidth, electrical & optical characterization, homogeneous irradiation
Rainbow set-up / cold halogen lamp (KL1500)	2	400 - 800	1	Localized wavelength dispersed, full spectrum
Laser 404nm (blue)	2000	404	0.3 - 3	High intensity, solely within absorption
Laser 532nm (green)	55000	532	7 – 30	High intensity, solely outside absorption
Inside PolyLED device	~ 10	400 - 620		

The experiments and the corresponding analysing methods, involving these three light sources and corresponding set-ups, are used in a way that the obtained results, as described in the previous chapter, are complementary and supportive to each other.

From this synergy of experiments and analyzing methods the main conclusion is that light emitted by today's blue PolyLED does contribute, to a certain degree, to its own degradation.

In section 2.4 (Parameter space of photo-degradation) the parameters of importance were mentioned. They are briefly discussed.

The degradation effects are different for irradiation with light of wavelengths within and outside the absorption band of the LEP, indicating different degradation mechanisms. Degradation of the device due to irradiation with light within the absorption band was expected because of interactions with the LEP itself, e.g. by formation of excitons. Degradation of the device due to irradiation with light outside the absorption band was rather unexpected and a degradation mechanism involving photo-absorption by the cathode is assumed.

From the results of the suntest experiments it became clear that changing the electrical state (OCP, Built-in, low Forward) during irradiation did not lead to a change in effects of photo-degradation. Since their lifetime curves behaved similar, the presence of charge carriers and excited states do not play a dominant role in the interactions with photons. Only the high Forward mode showed a different behaviour, but this may be understandable since under these circumstances the dominant degradation is caused by electrical stress and the device produces more photons by itself as with regard to the external light source. However, these experiments showed that the effects of electrical degradation and photo-degradation are not interchangeable and are likely to be caused by different mechanisms.

To study the mechanisms of photo-degradation during different stages in the lifetime of a display, only few experiments were done under not ideal experimental circumstances. Therefore they were not mentioned in chapter 5. However, they did show recognizable photo-degradation effects of initial offset and initial improved stability after irradiation occurring at advanced stages of the lifetime curve. More experiments are needed to confirm reproducibility of the effects and to draw final conclusions.

The amount of light during irradiation is of importance in the degradation effects. Most of the photo-degradation effects were already caused by limited amounts of irradiation. From the suntest experiments and the laser experiments saturation phenomena were observed for the longest irradiation times. Irradiation in the absorption band of the LEP in the suntest set-up (low intensity) showed a permanent change of lifetime characteristic and irradiation with the blue laser (high intensity) showed loss of photoluminescence of the LEP bulk. It is assumed that these to are linked together.

As a general interpretation of all the results and sub conclusions, it is now supposed that:

Irradiation with wavelengths within the absorption band causes a change in the electrical properties of the PolyLED, by deteriorating the mobility and/or injection of charge carriers, leading to a loss in efficiency.

Irradiation with wavelengths outside the absorption band causes a change in electrical properties of the PolyLED, by deteriorating the mechanism for charge carrier injection into the LEP.

From all the experiments together the idea is that in a normally operated PolyLED (where light is generated with wavelengths larger than 400nm) due to absorption of its own light additional excited states are generated in the LEP and [redacted]

To investigate these ideas in more detail more experiments are needed, especially concerning the nature of interactions involved with the interface between polymer layer and cathode. Also studies about changes in charge carrier mobility and injection due to photo-absorption could provide valuable information.

7. General conclusions

From the experiments it followed that visible light participates in the degradation process. Two regimes of light that contribute to the degradation of a blue PolyLED can be distinguished: light with wavelengths within the absorption band of the blue PolyLED and light with wavelengths outside of the absorption band. Since inside the blue PolyLED device, photons of both regimes are generated during normal operation, effects due to both of these regimes are applicable.

Irradiation of a blue LEP with photons outside the absorption band leads to an initial loss of luminance efficiency of the PolyLED together with an improved stability of its efficiency within the first few hours of operation after irradiation. These initial changes are cancelled out after a few hours of operation when compared to a non-irradiated PolyLED. [redacted]

The same initial changes apply to irradiation of a blue PolyLED with photons with wavelengths comparable to its own spectrum. However when irradiated further into the absorption band, the initial loss of luminance efficiency is more permanent, efficiency stability is less and overall lifetime decreases.

However, even in the absence of charge carriers and excited states (which normally are present in an operated device) the effects of photo-degradation due to irradiation are observed. The presence of the Ba/Al cathode is crucial for photons with energies outside the absorption band to contribute in a degradation process. Photons with energies corresponding to the absorption band of the PolyLED also interact with the bulk of the polymer whereas no proof of this has been found for photons with energies outside the absorption band.

These facts indicate that there are at least two mechanisms for degradation involving photons. Since wavelengths of both regimes are emitted by the PolyLED under normal operating conditions, both mechanisms are applicable and by emitting light the device contributes to its own degradation.

8. Literature

[1] H.Hoegl, *On Photoelectric Effects in Polymers and Their Sensitization by Dopants*, J. Phys. Chem. 69, 755 (1965).

[2] M.Pope, H.Kallmann, P.Magnante, *Electroluminescence in organic crystals*, J. Phys. Chem., 38, 2042 (1963)

[3] J.H.Burroughes et al., *Light-emitting diodes based on conjugated polymers*, Nature 347, 539-541 (1990).

[4] R.H.Friend et al., *Electroluminescence in conjugated polymers*, Nature 397, 121 - 128 (1999)

[5] R.E.Peierls, *Quantum Theory of Solids*, Oxford University Press, London, 1955

[6] W.Brütting, S.Berleb and A.G.Mückl, *Device physics of organic light-emitting diodes based on molecular materials,* Organic Electronics 2, 1-36, (2001)

[7] W.R.Salaneck and J.L.Brédas, *The metal-on-polymer interface in polymer light-emitting-diodes*, Adv. Mater. 8, 48-52, (1996). | ISI | ChemPort |

[8] W.R.Salaneck, S.Stafström and J.L.Brédas, *Conjugated Polymer Surfaces and Interfaces*, Cambridge Univ. Press, (1996).

[9] S.Vulto, M.Büchel, M.Kilitziraki, M.de Kok and E.Meulenkamp, Philips Research Technical Note 2003/00788

[10] E.A.Meulenkamp, Technical Note Philips Research (under preparation)

[11] Manual Atlas Suntest XLS/XLS+

[12] F.L.Pedrotti and L.S.Pedrotti, *Introduction to Optics (second edition)*, Prentice-Hall, (1993), Chapter 17

[13] C.Palmer, *Diffraction Gratings Handbook*, fifth edition, Thermo RGL, (2002)

[14] P.v.d.Weijer, E.Meulenkamp S.Vulto, B. Jacobs, M.Meulendijk, M.Kuilder and M.Kuyken, *Measurements on the Initial Drop of Light Emission during Operation of Polymer LEDs*, Philips Research Technical Note 2001/044

[15] P.v.d.Weijer, M.Kilitziraki, M.Kuilder, M.Ligter and M.Meulendijk, *Effect of driving on the stability of polymer Light Emitting Diodes*, Philips Research Technical Note 2003/00789

[16] S.Mensfoort, *Charge transport in and device characterization of blue polymer Light-Emitting Diodes*, master thesis Eindhoven University of Technology, (2005)

Acknowledgements

Now that the final report is finished, graduation knocks on the door. Reaching this point the way I did this last year was not possible without the help or support of several people. Here I would like to thank them.

First I like to thank my mentors at Philips Research and the TU/e, Ralph Kurt and Martijn Kemerink for the opportunity to do my graduation project at Philips and to work on an inspiring project. Ralph I would like to especially thank you for letting me follow my own line through the experimental research and for your critical and also enthusiastic approach, but also for the encouragement and opportunities to learn more about Philips and the industrial environment around research.

Next I would like to thank Michael Büchel for his help during the last part of my experimental research, his critical approach towards my report, even though I not always fully agreed at some points, and the discussions we had due to several complex results of some experiments.

Furthermore another big thank you to all the people form the Reliability Centre, where I did many experiments, for their cooperation, support, patience and humour. A special thank you to Martien Meulendijk and Marc Kuilder for helping me with my first experiments.

Also I like to thank all the people from the "Indigo-meetings", where I regularly presented and discussed my findings.

I would like to thank my roommates and fellow students at Philips for the many joyful times at the office and afterwards.

And last but not least I really want to thank my family, friends and roommates for their support during my study in Eindhoven at the TU/e.

Appendix

A Wavelength analysis by dispersion

As a basic theoretical background for the Rainbow set-up and its analyzing method a brief introduction to blazed diffraction gratings is presented. Basic grating theory is part of many fundamental optics books, like e.g. [12]. For more details special handbooks about gratings are available, like for instance [13].

Diffraction gratings are used to disperse light, i.e. to separate light of different wavelengths spatially. Irradiating for example a blue PolyLED sample with this wavelength-dispersed light opens one way of analysing the effects of different wavelengths or photon energies on the degradation of PolyLED samples.

Diffraction grating

A typical diffraction grating consists of an optically reflective substrate, with large number of parallel grooves ruled or replicated in its surface. These grooves can be considered as multiple slits in the Fraunhofer diffraction theory. From this the so called grating equation can be derived.

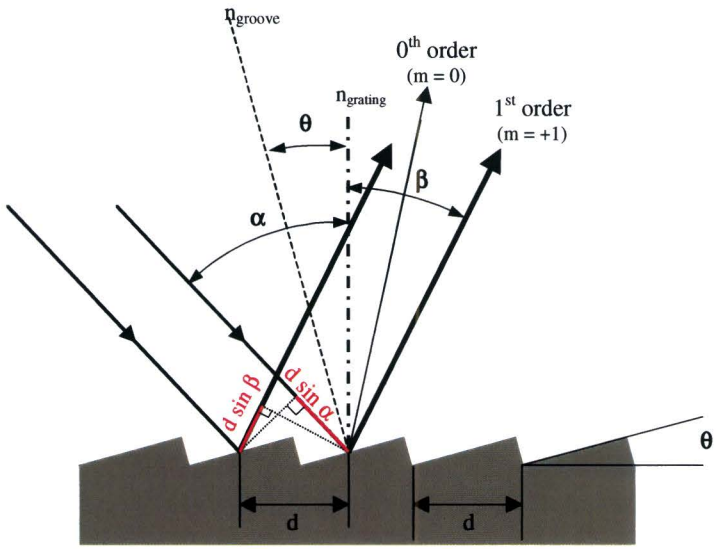

Figure 43: Neighbouring reflection grating grooves illuminated by monochromatic light incident at angle α with the grating normal. For light diffracted in the direction β the net path difference of the two waves is ΔS=d·(sinα ± sinβ). Only the first positive order (m=+1) is shown for clarity.

Figure 43 shows parallel light of a certain wavelength λ incident at an angle α to the grating normal onto two adjacent grooves. The path difference (ΔS) between light from adjacent grooves be can determined to be d·(sinα ± sinβ). The principle of interference dictates that light from adjacent grooves is in phase only when ΔS is equal to integral multiples of the wavelength, λ. So, the so called grating equation is:

$$d(\sin\alpha \pm \sin\beta) = m\lambda \qquad (1)$$

where m is the grating order, or spectral order. The plus/minus sign in equation (1) takes into account angles diffracted to the left or to the right of the normal reflection (0^{th} order), and the sign convention that is used.

In figure 43 only two grooves are considered. Including all the other grooves does not change the basic equation. In fact it even enhances the optical resolution of the system. The light is diffracted from the grating in several directions corresponding to the orders m = -3, -2, -1, 0, 1, 2, 3, etc.

When a parallel beam of polychromatic light is incident on a grating then the light is dispersed so that each wavelength satisfies the grating equation. This is shown in figure 44, but only for order m = +1, +2, +3.

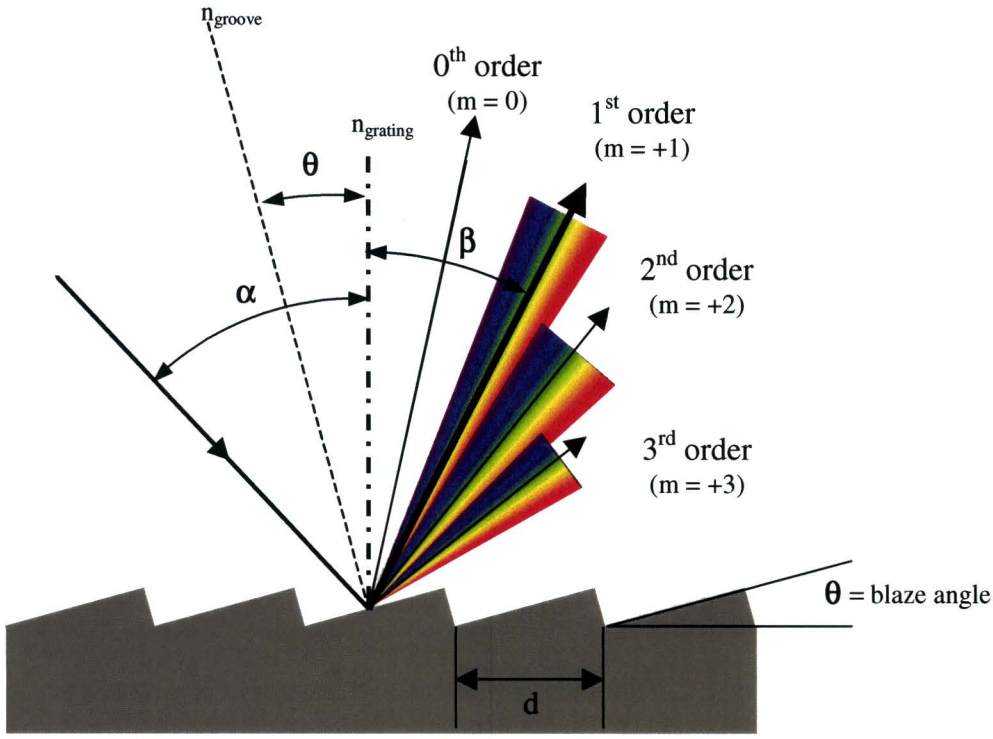

Figure 44: Schematic representation of a polychromatic dispersion on a reflective diffraction grating. Note that only the positive orders are shown and at different distances for reasons of clarity.

Also schematically shown is the angular spread of the orders. The non-overlapping wavelength range in a particular order is called the free spectral range, F. Overlapping occurs because in equation (1) the product d·sinβ may be equal to several possible combinations of mλ. This leads to the following expression of F:

$$m\lambda_2 = (m+1)\lambda_1 \quad \Rightarrow \quad \lambda_2 - \lambda_1 = F = \frac{\lambda_1}{m} \qquad (2)$$

where λ_2 is the longest non overlapping wavelength in order m
λ_1 is the shortest detectable wavelength

This expression then determines if and what kind of bandwidth filters should be used for appropriate wavelength analysis, given the groove density 1/d for the used grating. Also, the irradiance in each order falls down rapidly with increasing order, so any mixing of light from neighbouring orders should be rather small.

Efficiency and blazing

The efficiency of a grating is generally not the same for different wavelengths. So, for analysis the wavelength dependence was measured. The absolute efficiency of a grating in a given wavelength region and order is the ratio of the diffracted light energy to the incident light energy in the same wavelength region. Increasing the number of grooves on a grating, for example, increases the light energy throughput. A grating is most efficient when the rays emerge from the grating as if by direct reflection of the facets of which the grating is composed. By changing the angle θ of the facets the diffraction maximum can be shifted from the 0^{th} order into another order. This technique is called blazing and maximum use of this effect acquires the right conditions.

Figure 45 shows an idealized blaze efficiency function for a grating blazed at wavelength λ_B in first order (m=1) [13].

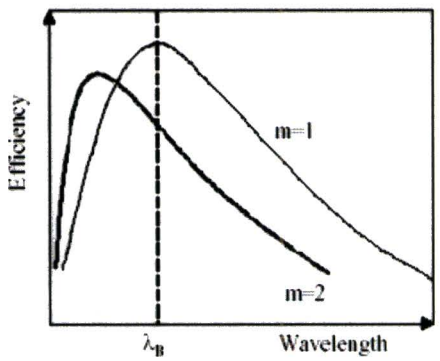

Figure 45: Typical relationship between efficiency and wavelength for a blazed diffraction grating as function of interference order. λ_B is the so called blaze wavelength where the efficiency curve of a particular order reaches its maximum.

For very low blaze angle gratings ($\theta < 5°$) a simple picture of blazing is applicable, in which each groove facet can be considered a simple flat mirror. The diffracted efficiency is greatest for that wavelength that is diffracted by the grating in the same direction as it would be reflected by the facets.

B Estimation radiation power PolyLED

Estimation of the external radiance power generated in a PolyLED.

$$Q_{eff.external} = \frac{\#\,photons}{\#\,injected\ charge\ carriers} \times optical\ outcoupling\ factor \qquad (3)$$

$$E_{photon} = \frac{hc}{\lambda} \qquad (4)$$

Measured boundary conditions:

$Q_{eff.external} \approx 1\% - 4\%$, typical for PolyLEDs

Current density = 2.5mA = $2.5 \cdot 10^{-3}$ C/s

Fundamental physical constants:

e = $1.60 \cdot 10^{-19}$ C
h = $6.63 \cdot 10^{-34}$ Js
c = $3.00 \cdot 10^{8}$ m/s

Calculated using equation (3) and (4):

Number of photons with Q_{eff} =1% and current=2.5mA: $1.6 \cdot 10^{14}$ photons

Corrected for the spectral power distribution of the LEP this corresponds to a total of 0.07mW (integral over its whole spectrum from 380nm to 780nm as illustrated in figure 17).

Assume:

Optical outcoupling factor: 4. From optical simulations it is known that the light emitted in the LEP is a factor 3 to 4 larger than what is coupled out of the device.

$Q_{eff.external}$: factor 1-4

Typically the pixel with an area of 9mm² is of interest

Conclusion of estimation:

Radiation power inside PolyLED: ~ 10mW/cm².

Lowest estimation: 3mW/cm² (=0.07 × 4 × 1 / 0.09)

Highest estimation: 12mW/cm² (=0.07 × 4 × 4 / 0.09)